DETERMINATION OF STOCHASTIC MODEL PARAMETERS OF INERTIAL SENSORS

A THESIS SUBMITTED TO
THE GRADUATE SCHOOL OF NATURAL AND APPLIED SCIENCES
OF
MIDDLE EAST TECHNICAL UNIVERSITY

BY

ALPER ÜNVER

IN PARTIAL FULFILLMENT OF THE REQUIREMENTS
FOR
THE DEGREE OF DOCTOR OF PHILOSOPHY
IN
ELECTRIC ELECTRONIC ENGINEERING

JANUARY 2013

Approval of the thesis:

DETERMINATION OF STOCHASTIC MODEL PARAMETERS OF INERTIAL SENSORS

submitted by **ALPER ÜNVER** in partial fulfillment of the requirements for the degree of **Doctor of Philosophy in Electric Electronic Engineering Department, Middle East Technical University** by,

Prof. Dr. Canan Özgen _____
Dean, Graduate School of **Natural and Applied Sciences**

Prof. Dr. İsmet Erkmen _____
Head of Department, **Electric Electronic Engineering**

Prof. Dr. Mübeccel Demirekler _____
Supervisor, **Electric Electronic Engineering, Dept. METU**

Examining Committee Members:

Prof. Dr. Kemal Leblebicioğlu _____
Electric Electronic Engineering Dept., METU

Prof. Dr. Mübeccel Demirekler _____
Electric Electronic Engineering Dept., METU

Prof. Dr. Tolga Çiloğlu _____
Electric Electronic Engineering Dept., METU

Asist. Prof. Dr. Yakup Özkazanç _____
Electric Electronic Engineering Dept., Hacettepe Üniversity

Assoc. Prof. Dr. Emre Tuna _____
Electric Electronic Engineering Dept., METU

Date: *30 January 2013*

I hereby declare that all information in this document has been obtained and presented in accordance with academic rules and ethical conduct. I also declare that, as required by these rules and conduct, I have fully cited and referenced all material and results that are not original to this work.

Name Surname: Alper ÜNVER

Signature:

ABSTRACT

DETERMINATION OF STOCHASTIC MODEL PARAMETERS OF INERTIAL SENSORS

Ünver, Alper

PhD, Department of Electric Electronic Engineering

Supervisor: Prof. Dr. Mübeccel Demirekler

January 2013, 82 pages

Gyro and accelerometer systematic errors due to biases, scale factors, and misalignments can be compensated via an on-board Kalman filtering approach in a Navigation System. On the other hand, sensor random noise sources such as Quantization Noise (QN), Angular Random Walk (ARW), Flicker Noise (FN), and Rate Random Walk (RRW) are not easily estimated by an on-board filter, due to their random characteristics.

In this thesis a new method based on the variance of difference sequences is proposed to compute the powers of the above mentioned noise sources. The method is capable of online or offline estimation of stochastic model parameters of the inertial sensors. Our aim in this study is the estimation of ARW, FN and RRW parameters besides the quantization and the Gauss-Markov noise parameters of the inertial sensors.

The proposed method is tested both on the simulated and the real sensor data and the results are compared with the Allan variance method. Comparison shows very satisfactory results for the performance of the method. Computational load of the new method is less than the computational load of the Allan variance on the order of tens.

One of the usages of this method is the individual noise characterization. A noise, whose power spectral density has a constant slope, can be identified accurately by the proposed method. In addition to this, the parameters of the GM noise can also be determined.

Another idea developed here is to approximate the overall error source as a combination of ARW and some number of GM sources only. The reasons of selecting such a structure is the feasibility of using these models in a Kalman filter framework for error propagation as well as their generality of modeling other noise sources.

Keywords: Angle Random Walk (ARW), Rate Random Walk (RRW), Flicker (1/f) Noise, Quantization Noise (QN), Gauss-Markov Noise, Allan Variance, Online Parameter Estimation.

ÖZ

ATALETSEL ÖLÇERLERİN STOKASTİK MODEL PARAMETRELERİNİN BELİRLENMESİ

Ünver, Alper

Doktora, Elektrik Elektronik Mühendisliği Bölümü

Tez Yöneticisi : Prof. Dr. Mübeccel Demirekler

Ocak 2013, 82 sayfa

Dönüölçer ve ivmeölçerin sabit kayma, orantı katsayısı açı kayma hatalarından kaynaklı sistamatik hataları seyrüsefer sistemlerinde gerçek zamanlı çalışan Kalman filtre yaklaşımı ile giderilebilmektedir. Diğer yandan nicemleme, açısal rastgele yürüme, sabit kayma kararsızlığı ve açısal hız rastgele yürüme hataları rastgele yapısından dolayı kolaylıkla kestirelemez.

Bu tezde fark dizilerinin varyansına dayanan ve yukarıda bahsi geçen stokhastik hata kaynaklarının gücünü hesap eden yeni bir yöntem önerilmektedir. Bu metod ile ataletsel ölçerlerin stokhastik hata kaynakları eşzamanlı veya ard işlemleme ile hesap edilebilmektedir. Bu çalışmaaki amacımız ataletsel ölçerlerin açısal rastgele yürüme, sabit kayma kararsızlığı ve açısal hız rastgele yürüme hatalarının yanısıra Gauss Markov ve nicemleme hata parametrelerinin kestirilmesidir.

Önerilen metod benzetim ve gerçek ataletsel ölçer verileri kullanılarak ve test edilip, sonuçlar Allan variance yöntemi ile karşılaştırılmıştır. Karşılaştırmalar sonucunda önerilen metodun performansına ilişkin çok iyi sonuçlar bulunmuştur.Önerilen metodun hesaplama yükü Allan varyans yöntemine gore 10 katlar mertebesinde daha azdır.

Tek bir gürültü kaynağının karekterizasyonu bu metod kullanılarak gerçekleştirilebilir. Güç tayf yoğunluğunda sabit eğime sahip gürültülerin önerilen metod ile tüm parametreleri kestirilebilir. Gürültü kaynağının Gauss Markov olduğu biliniyorsa bu gürültüye ait de bütün parametreler kestirilebilir.

Bu çalışmada geliştirilen bir başka fikirde bütün hata kaynaklarını açısal rasgele yürüme ve birkaç Gauss Markov hata modeli ile karakterize etmektir.Bu yapısal seçimdeki en önemli neden Kalman filtre yapısındaki hata ilerlemelerine uyumluluk ile Gauss Markov hata kanağının diğer hata kaynaklarını modellemek için uygunluğudur.

Anahtar Kelimeler: Açısal Rasgele Yürüme, Flicker Gürültüsü, Hız Rasgele Yürüme, Allan Variance, Gerçek Zamanlı Kestirim

To my father, İsmail ÜNVER

ACKNOWLEDGMENTS

I would like to express my sincere gratitude to Prof Dr. Mübeccel DEMİREKLER for her endless support, guidance and for helpful discussions we have made throughout the study.

This work has been supported by TÜBİTAK-SAGE and ASELASAN. I would like to thank TÜBİTAK-SAGE and ASELSAN for providing the computational power and literature sources which were enormously important for this study.

I would like to thank my colleagues Dr. Burak KAYGISIZ and Dr. Yüksel SUBAŞI for their unforgettable valuable teamwork and help in my studies.

My special thanks go to my mother, Hanife ÜNVER, my father İsmail ÜNVER and my brother Mehmet Emin ÜNVER, for their endless support.

Lastly, my deepest thanks go to my wife and two daughters who gave me endless support and love which made this thesis possible.

TABLE OF CONTENTS

LIST OF FIGURES

FIGURES

LIST OF TABLES

TABLES

CHAPTER 1

INTRODUCTION

Because of their high speed and reliability to external disturbances, inertial navigation systems are one of the most important sources for navigation solutions. Main drawback of inertial systems is the increase of their error with time unboundedly. Therefore gyroscope and accelerometer error sources used in an inertial navigation system must be modeled and compensated, if possible, so that navigation performance can be estimated and increased. Inertial sensor models include both deterministic and stochastic error sources. Deterministic error sources, namely bias, scale factor and misalignment errors, can be determined and compensated at the output of the sensors with well known methods [3]. On the other hand stochastic error sources like Quantization Noise (QN), Angle Random Walk (ARW), Gauss-Markov (GM) noise, Bias Instability, sometimes called flicker noise (BI), and Rate Random Walk (RRW) are not easy to estimate and compensate.

Allan variance method is a very powerful tool for the discrimination and the evaluation of stochastic error sources ([3], [8]). However obtaining the error source parameters by using this method requires too much data to be acquired and too many calculations to be done.

Other than the Allan variance method, few studies exist in the literature about the online estimation of the error parameters. The online estimation of Allan variance parameters for the case of the existence of only Angle Random Walk and Rate Random Walk error sources is studied in [2]. This study uses finite dimensional filters for maximum likelihood estimation of discrete Gauss Markov models, [1], [4], [10]. However the effectiveness and the performance of the algorithm degrade in the case of the existence of other stochastic noise sources. [16] extends the model to include Bias Instability noise term as a first order GM noise. Similarly, in [12], Allan variance is used to determine the model parameters of ARW, RRW and BI noise sources using the synthetic data only. Bias instability is modeled as a first order GM noise in this study.

Because of the non-rational transfer function of bias instability, it is modeled by different techniques in the literature. In [13] this noise, denoted by $x[n]$, is generated using the inverse Fourier transform of a sequence of two random processes $G(n)$ and $U(n)$ where $G(n)$ is Gaussian and $U(n)$ is uniformly distributed on the interval [0, 2π]. The related expression is given in (1). In this formulation β can be thought as a spectral parameter and is equal to one for the bias instability noise.

$$x[n] = \mathrm{Re}\left(IFFT\left(\sum_{n=1}^{M} G(n) n^{\frac{\beta}{2}} \left\{ \cos(2\pi U(n)) + j \sin(2\pi U(n)) \right\} \right) \right) \qquad (1)$$

For navigation purposes, high frequency noise is considered to be ARW (white noise) and low frequency part is modeled as a first or higher order GM noise. In [14], it is shown that second or third order AR modeling of low frequency noise gives better results than the first order GM modeling. A multi-resolution technique is suggested in this study in order to increase the navigation performance. In this way wideband white noise is aimed to be removed from the sensor output.

Using de-noising techniques is another approach of handling the stochastic noises of inertial sensors. In [15], Kaiser Window based FIR low pass filter and in [17], Neural Network Model are used for this purpose. This approach suffers from the bandwidth problems. In order to use them useful bandwidth of the sensor for the specific application must be identified.

The originality of our work is to include almost all possible stochastic error sources into the identification problem and solve the problem in an efficient way by proposing a new method which is much faster and requires less memory compared to the Allan variance method. Proposed method is based on the calculation of the variances of the differences of sensor outputs and their delayed versions. Second order statistics of difference sequences depend on the error source coefficients differently for each delay time. The difference sequence obtained from the sensor output that includes the five basic stochastic error sources is stationary. Therefore, the variance of it depends only the parameters of the unknown noise parameters and the amount of delay used in the difference operation.

For a tactical grade navigation system, besides the angle and the rate random walk parameters bias instability is one of the most important parameter that must be determined. For this noise term, different modeling techniques are examined in [6] and [7]. The noise model given in [6] is used in this study because of the suitability of it to the proposed algorithm. The aim of this study is to determine these three parameters together with the GM and the quantization noise coefficients. Rate ramp parameter which can be determined by using the Allan variance is not included into our model. However our model can easily be extended to include it.

One of the applications of the proposed method is the characterization of the noise source that has a constant slope in the power spectral density function. These types of noise sources can be modeled in discrete time by filtering the white noise with a rational or non-rational transfer function, depending on the value of α, of the form $H(z) = \dfrac{1}{\left(1 - z^{-1}\right)^{\frac{\alpha}{2}}}$. There are too many noise sources that can be classified in this category. All of the noise sources other than the GM noise specified in this study are in this form. The value of α is -2 for QN, zero for ARW, 1 for BI and 2 for RRW noises. The method proposed in this study is not only applicable for the specified noise sources but also suitable for all $1/f^{\alpha}$ type noise sources for $|\alpha| \leq 2$. Once the characteristics of the noise is determined by finding the parameter α, power of the white noise input is found by least squares method and the noise is identified completely. If the noise type is a first order GM noise, then the method proposed can be used with a slight modification, made for the determination of the GM noise parameters.

Another idea developed here is to approximate the overall error sources as a combination of ARW and some number of GM noises only. The reasons of selecting such a structure is the feasibility of using these models in a Kalman filter framework for error propagation as well as their generality of modeling other noise sources. The idea is exploited by generating estimation techniques that use 2 and 3 models. Results are obtained for the real sensor data.

The performance of the method is tested both by using the simulated and the real data. When using real data, performance is tested by comparing the Allan variance of the original data with the Allan variance obtained from the synthetic data generated by the estimated parameters.

The organization of the thesis is as follows. Allan variance method is explained in Chapter 2 for the sake of completeness. In Chapter 3 the systematic and the stochastic error models for inertial sensors are given. In this chapter bias Instability (flicker noise) is modeled as the output of a system with a non-rational transfer function which is approximated by a finite number of terms of its Taylor series expansion. The method proposed in this thesis is fully explained with mathematical proofs in Chapter 4. In Chapter 5 simulations and results are given and compared with the Allan variance method. The proposed method is also applied to real accelerometer data of approximately 7 hours taken at 10 Hz sampling frequency.

The two different application of the proposed algorithm is given in Chapter 7 and Chapter 8. In Chapter 7, the individual noise characterization is explained. By simulations it is shown that if there is only one noise source and if its type is classified as GM or not GM, then the proposed algorithm determines the noise parameters accurately and effectively. In Chapter 8, sensor output is modeled using the ARW and GM noise sources only. Number of GM noise sources is selected as one or two in two different cases. For the two GM noise source case correlation times of the two models are forced to belong to two different non overlapping regions. Experimental results show that both with simulated and real data the method are quite satisfactory for the sensor stochastic error characterization.

Finally, conclusions of the study and future works are given in Chapter 9.

CHAPTER 2

ALLAN VARIANCE AND STOCHASTIC ERROR PARAMETERS OF INERTIAL SENSOR

2.1 Allan Variance Background

Allan variance is first introduced to characterize the phase and frequency instability of precision oscillators [3]. It is a time domain analysis technique. Independent noise sources can be identified from the log-log plot of the square root of it versus correlation time. This time domain analysis technique is easy to use. Once it is evaluated, different characteristics of the noise sources are differentiated either from the slope of the curve or the sinusoidal shape of it. The quantization, ARW, BI, RRW and rate ramp noises generate different slopes in the "square root of the Allan variance" curve while GM noise and/or sinusoidal noise introduce a sinusoidal shape in it. The success of this technique depends on the assumption that the effect of all noise sources becomes active at different correlation times of the Allan variance plot.

Besides all the noise variances, correlation time of GM noise and the frequency of the sinusoidal noise are also determined by the Allan variance method. In other words all the noise sources can be characterized completely.

Evaluation of Allan variance from the N samples of the data with a sampling period of τ_0 is explained below. Note that the time interval of the overall data is $N\tau_0$.

Data clusters of lengths 1, 2, …, M ($M < \frac{N}{2}$) are formed. Allan variance is a function of M for each cluster. Averages are obtained for the clusters over the length of that cluster. Note that there are $K = N/M$ clusters.

$$\underbrace{\omega_1, \omega_2, ..., \omega_M}_{\mathrm{k}=1}, \underbrace{\omega_{M+1}, ..., \omega_{2M}}_{\mathrm{k}=2}, ..., \underbrace{\omega_{N-M+1}, ..., \omega_N}_{\mathrm{k}=K}$$

Then the average of each cluster is evaluated as in (24).

$$\bar{\omega}_k(M) = \frac{1}{M}\sum_{i=1}^{M} \omega_{(k-1)M+i} \tag{2}$$

The Allan variance can be calculated as given below.

$$\sigma^2(\tau_M) = \frac{1}{2}\left\langle \left(\bar{\omega}_{k+1}(M) - \bar{\omega}_k(M)\right)^2 \right\rangle$$
$$= \frac{1}{2(K-1)} \sum_{k=1}^{K-1} \left(\bar{\omega}_{k+1}(M) - \bar{\omega}_k(M)\right)^2 \quad (3)$$

where, $\tau_M = M\tau_0$.

The symbol $\langle x \rangle$ denotes the mean of x. The relationship between Allan variance and the two-sided PSD is given in (26).

$$\sigma_\Omega^2(\tau_M) = 4\int_0^\infty S_w(f) \frac{\sin^4(\pi f \tau_M)}{(\pi f \tau_M)^2} df \quad (4)$$

where $S_w(f)$ is the PSD of the given data. This equation is the key result that will be used to calculate the Allan variance [3].

2.2 Allan Variance and Power Spectral Density

The five basic noise terms in an inertial sensor system are angle random walk (white noise), rate random walk (Brownian motion), bias instability (flicker noise), quantization noise, and Gauss Markov noise.

The Allan variance obtained by performing the prescribed operations, is related to the PSD of the noise terms in the original data set as given in (26).

An interpretation of this expression is that the Allan variance is proportional to the total noise power of the gyro rate output when passed through a filter with the transfer function of the form $\frac{\sin^4(x)}{x^2}$. This particular transfer function is the result of the method used to create and operate on the clusters [3]. When the argument, x, of this transfer function scaled by a positive number greater than one the function becomes narrow and close to the origin.

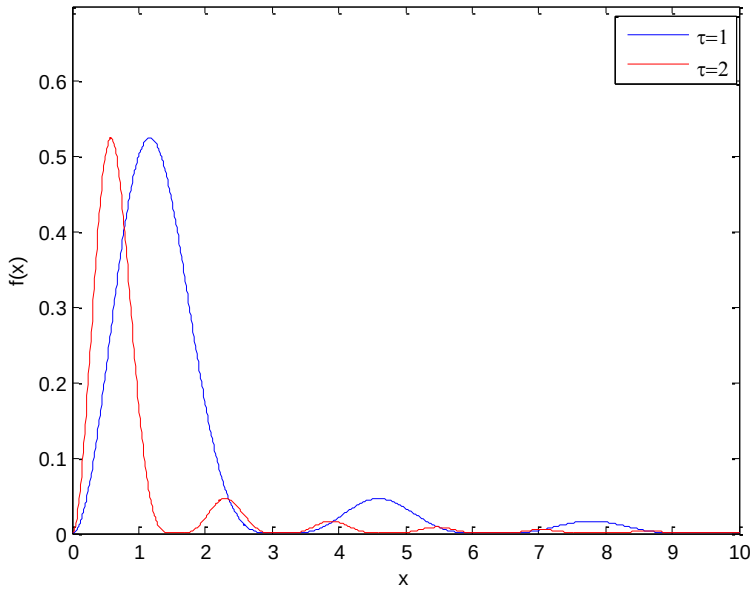

Figure 1: f(x) =sin^4(τx)/ (τx)^2 plots for τ=1 (Blue) andτ=2 (Red)

It is seen from this equation and from Figure 1 that the filter pass-band depends on the correlation time τ. This suggests that different types of random processes can be examined by adjusting the filter pass band by varying τ. Thus, the Allan variance provides a means of identifying and quantifying various noise terms that exist in the data. It is normally plotted as the square root of the Allan variance versus τ on a log-log plot.

2.3 Derivation of the Allan Variance

The Power Spectral Density (PSD) of a signal is important to characterize and determine the stochastic error model parameters of the inertial sensors. PSD is calculated by taking the Fourier transform of the autocorrelation function of the sensor output. Allan variance is another technique that is used for the same purpose. The aim of this section is to derive the relationship between these approaches. Although the relationship is used widely in the literature its derivation is not so common. We give a simple and easily understandable derivation here for the sake of completeness.

Equation (26) gives the Allen variance in terms of PSD. This operator is not injective, i.e., its inverse does not exist. To show the equality we first begin by the definition of the right side it.

$$\sigma_{\Omega}^{2}(\tau)=\frac{1}{2}\left\langle \overline{\omega}_{k+1}-\overline{\omega}_{k}\right\rangle^{2} \tag{5}$$

where, $\langle\ \rangle$ is used for the expected average, and τ is used for cluster length. The cluster average is computed as given below.

$$\overline{\omega}_{k}=\frac{1}{M}\sum_{i=1}^{M}\omega_{(k-1)M+i}=\frac{1}{\tau}\int_{t_k}^{t_k+\tau}\omega(t)dt \tag{6}$$

where, $\omega(t)$ is inertial sensor output waveform in the continuous time domain. The Allan variance can be written as;

$$\sigma_{\Omega}^2(\tau)=\frac{1}{2}\left\{\left\langle\overline{\omega}_{k+1}^2\right\rangle^2-2\left\langle\overline{\omega}_{k+1}\overline{\omega}_k\right\rangle^2+\left\langle\overline{\omega}_k^2\right\rangle^2\right\} \tag{7}$$

$\left\langle\overline{\omega}_k^2\right\rangle$ can be expressed in terms of the continuous inertial sensor output so that the Autocorrelation function and PSD expressions are formed.

$$\left\langle\overline{\omega}_k^2\right\rangle=\frac{1}{\tau^2}\int_{t_k}^{t_k+\tau}dt\int_{t_k}^{t_k+\tau}dt'\left\langle\omega(t)\omega(t')\right\rangle=\frac{1}{\tau^2}\int_{t_k}^{t_k+\tau}dt\int_{t_k}^{t_k+\tau}dt'R_{\omega}(t-t') \tag{8}$$

$R_{\omega}(\tau)$ is the autocorrelation function of the inertial sensor output and it is equal to inverse Fourier transform of the PSD. Therefore,

$$\begin{aligned}
\left\langle\overline{\omega}_k^2\right\rangle&=\frac{1}{\tau^2}\int_{t_k}^{t_k+\tau}dt\int_{t_k}^{t_k+\tau}dt'\int_{-\infty}^{\infty}S_{\omega}(f)e^{j2\pi f(t-t')}df\\
&=\frac{1}{\tau^2}\int_{-\infty}^{\infty}dfS_{\omega}(f)\int_{t_k}^{t_k+\tau}dt\int_{t_k}^{t_k+\tau}dt'e^{j2\pi f(t-t')}\\
&=\frac{1}{\tau^2}\int_{-\infty}^{\infty}dfS_{\omega}(f)\left(\frac{1}{j2\pi f}\left(e^{j2\pi f(t_k+\tau)}-e^{j2\pi ft_k}\right)\right)\left(\frac{1}{j2\pi f}\left(e^{-j2\pi ft_k}-e^{-j2\pi f(t_k+\tau)}\right)\right)\\
&=\frac{1}{\tau^2}\int_{-\infty}^{\infty}dfS_{\omega}(f)\left(\frac{1}{j2\pi f}\frac{1}{j2\pi f}\left(e^{j2\pi f\tau}-2+e^{-j2\pi f\tau}\right)\right)\\
&=\frac{1}{\tau^2}\int_{-\infty}^{\infty}dfS_{\omega}(f)\frac{1}{(\pi f)^2}\left(\frac{e^{j\pi f\tau}-e^{-j\pi f\tau}}{2j}\right)^2\\
&=\int_{-\infty}^{\infty}dfS_{\omega}(f)\left[\frac{\sin^2(\pi f\tau)}{(\pi f\tau)^2}\right]
\end{aligned} \tag{9}$$

Similarly,

$$\left\langle\overline{\omega}_k\overline{\omega}_{k+1}\right\rangle=\frac{1}{\tau^2}\int_{t_k}^{t_k+\tau}dt\int_{t_k+\tau}^{t_k+2\tau}dt'\left\langle\omega(t)\omega(t')\right\rangle=\frac{1}{\tau^2}\int_{t_k}^{t_k+\tau}dt\int_{t_k+\tau}^{t_k+2\tau}dt'R_{\omega}(t-t') \tag{10}$$

and,

$$
\begin{aligned}
\left\langle \overline{\omega}_k \overline{\omega}_{k+1} \right\rangle &= \frac{1}{\tau^2} \int_{t_k}^{t_k+\tau} dt \int_{t_k+\tau}^{t_k+2\tau} dt' \int_{-\infty}^{\infty} S_\omega(f) e^{j2\pi f(t-t')} df \\
&= \frac{1}{\tau^2} \int_{-\infty}^{\infty} df S_\omega(f) \int_{t_k}^{t_k+\tau} dt \int_{t_k+\tau}^{t_k+2\tau} dt' e^{j2\pi f(t-t')} \\
&= \frac{1}{\tau^2} \int_{-\infty}^{\infty} df S_\omega(f) \left(\frac{1}{j2\pi f} \left(e^{j2\pi f(t_k+\tau)} - e^{j2\pi f t_k} \right) \right) \left(\frac{1}{j2\pi f} \left(e^{-j2\pi f(t_k+\tau)} - e^{-j2\pi f(t_k+2\tau)} \right) \right) \\
&= \frac{1}{\tau^2} \int_{-\infty}^{\infty} df S_\omega(f) \left(\frac{1}{j2\pi f} \frac{1}{j2\pi f} \left(e^{j2\pi f\tau} - 2 + e^{-j2\pi f\tau} \right) \right) e^{-j2\pi f\tau} \\
&= \frac{1}{\tau^2} \int_{-\infty}^{\infty} df S_\omega(f) \frac{1}{(\pi f)^2} \left(\frac{e^{j\pi f\tau} - e^{-j\pi f\tau}}{2j} \right)^2 e^{-j2\pi f\tau} \\
&= \int_{-\infty}^{\infty} df S_\omega(f) \left[\frac{\sin^2(\pi f\tau)}{(\pi f\tau)^2} \right] e^{-j2\pi f\tau}
\end{aligned}
\tag{11}
$$

Using the Allan variance equation and the expression obtained above;

$$
\begin{aligned}
\sigma_\Omega^2(\tau) &= \frac{1}{2} \left\{ \left\langle \overline{\omega}_{k+1}^2 \right\rangle^2 - 2 \left\langle \overline{\omega}_{k+1} \overline{\omega}_k \right\rangle^2 + \left\langle \overline{\omega}_k^2 \right\rangle^2 \right\} \\
&= \frac{1}{2} \left\{ \left\langle \overline{\omega}_{k+1}^2 \right\rangle^2 + \left\langle \overline{\omega}_k^2 \right\rangle^2 \right\} - \left\langle \overline{\omega}_{k+1} \overline{\omega}_k \right\rangle^2 \\
&= \int_{-\infty}^{\infty} df S_\omega(f) \left[\frac{\sin^2(\pi f\tau)}{(\pi f\tau)^2} \right] - \int_{-\infty}^{\infty} df S_\omega(f) \left[\frac{\sin^2(\pi f\tau)}{(\pi f\tau)^2} \right] e^{-j2\pi f\tau} \\
&= \int_{-\infty}^{\infty} df S_\omega(f) \left[\frac{\sin^2(\pi f\tau)}{(\pi f\tau)^2} \right] \left(1 - e^{-j2\pi f\tau} \right)
\end{aligned}
\tag{12}
$$

Note that,

$$
\begin{aligned}
&\left(1 - e^{-j2\pi f\tau}\right) = \left(1 - e^{-j\pi f\tau}\right)\left(1 + e^{-j\pi f\tau}\right) \\
&= \left(1 - \cos(\pi f\tau) + j\sin(\pi f\tau)\right)\left(1 + \cos(\pi f\tau) - j\sin(\pi f\tau)\right) \\
&= 1 + \cos(\pi f\tau) - j\sin(\pi f\tau) - \cos(\pi f\tau) - \cos^2(\pi f\tau) + j\cos(\pi f\tau)\sin(\pi f\tau) \\
&+ j\sin(\pi f\tau) + j\cos(\pi f\tau)\sin(\pi f\tau) + \sin^2(\pi f\tau) \\
&= 2\sin^2(\pi f\tau) + j2\sin(\pi f\tau)\cos(\pi f\tau)
\end{aligned}
\tag{13}
$$

Therefore,

$$\sigma_{\Omega}^{2}(\tau) = 2\int_{-\infty}^{\infty} df S_{\omega}(f)\left[\frac{\sin^{4}(\pi f\tau)}{(\pi f\tau)^{2}}\right] + j2\int_{-\infty}^{\infty} df S_{\omega}(f)\cos(\pi f\tau)\left[\frac{\sin^{3}(\pi f\tau)}{(\pi f\tau)^{2}}\right]$$
$$= 4\int_{0}^{\infty} df S_{\omega}(f)\left[\frac{\sin^{4}(\pi f\tau)}{(\pi f\tau)^{2}}\right] \quad (14)$$

For a real data sequence $S_{\omega}(f)$ is even and the second integral becomes zero.

2.4 Typical Allan Variance Plot

Root Allan variance plot is used to determine the noise parameters of the sensor output by examining the corresponding slope i.e. -1 for quantization, -½ for angle random walk, zero for bias instability, ½ for rate random walk noise sources, or by finding the local maximum for Gauss-Markov noise. Both the value of Allan variance and the corresponding time are necessary in determination of input noise powers and the Gauss-Markov correlation time, [3].

An inertial sensor output data, whose input noise parameters are given in Table I, is generated during 55 hours simulation time with 0.1 second sampling period.

Table I: Input Noise Parameters

Parameters	ARW	BI	RRW	QN	GM
Input Noise Variances	1.9	1	0.0002	0.01	3 (Tc=7 sec)

In the Root Allan variance plot the specified points shown with the arrows are used to identify the input noise powers.

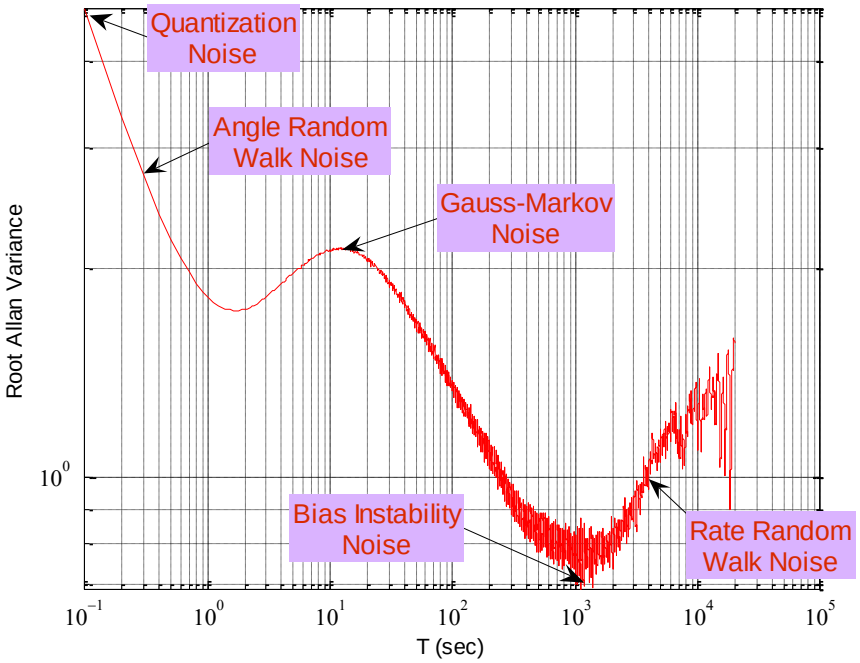

Figure 2: Typical Allan Variance Plot

CHAPTER 3

INERTIAL SENSOR MODELING AND ESTIMATION OF ITS RANDOM NOISE SOURCES

Inertial navigation system performance is highly related with the accuracy of inertial sensors, gyroscopes and accelerometers. Each sensor has different error sources and their value together with repeatability performances determine the accuracy. Generally, inertial sensor errors can be grouped as systematic and stochastic errors. Systematic errors can be detected and corrected more easily compared to the stochastic errors. In any application it is advised to correct the systematic errors before handling the stochastic errors. In this chapter we will first briefly explain the systematic errors then give more detailed explanations for the stochastic errors.

3.1 Systematic Error Model of Inertial Sensors

Scale factor, bias and misalignment errors are the main sources of the systematic errors of an inertial sensor. In order to determine the error model parameters of an inertial sensor it is usually forced with a deterministic input. The corresponding output and the known deterministic input are used to identify the unknown parameters.

Systematic error model of mechanical inertial sensors, such as a single or two degrees of freedom spinning wheel gyroscope or a pendulum accelerometer, includes second and even third order nonlinearities [3]. These parameters are determined similarly like the previous model parameters.

For mechanical sensors, dynamic response may be very critical depending on the application. In order to determine the bandwidth and the damping coefficient of the sensor, sinus sweep or white noise vibration input is usually applied as a sensor input.

Ignoring the environmental effects and the dynamic structure of the model, i.e. reducing it to a static one, accelerometer and gyroscope systematic errors can be modeled as in (15) and (16), [8].

$$\frac{E}{K_1} = K_0 + a_i + K_2 a_i^2 + K_3 a_i^3 + K_{ip} a_i a_p + K_{io} a_i a_o + K_{op} a_o a_p + \delta_o a_p - \delta_p a_o + \quad (15)$$

Where the subscript ‘i’ denotes the ‘input’, and ‘o’ denotes the output, ‘p’ the pendulum axis which is orthogonal to the input and the output axis. The other parameters are defined below.

E : Electrical output of accelerometer

K_1 : Scale Factor

K_0 : Bias

a_x : Inertial acceleration along x direction

K_2 : Second order nonlinearity (source of vibration rectification error)

K_3 : Third order nonlinearity coefficient

K_{xy} : Cross axes sensitivities

δ_x : Misalignment between x axis and input axis

$$\frac{E_i}{K_i} = \omega_i + b_i + G_i a_i + G_o a_o + G_s a_s + G_{io} a_i a_o + G_{is} a_i a_s + G_{os} a_o a_s + \delta_{io} \omega_o + \delta_{is} \omega_s + \quad (16)$$

The subscripts 'i' and 'o' denote the input and the output as before. 's' denotes the spin axis which is orthogonal to the input and the output axis. The parameters that are not defined above are the following.

K_i : Scale Factor corresponding to the input axis

b_i : Bias along the input axis

ω_x : Inertial angular input along x direction

G_x : Acceleration sensitivity along x direction

G_{xx} : Cross axes acceleration sensitivity

δ_{xi} : Misalignment between x axis and the input axis

Generally the second order and the third order effects are not included into the systematic error models and they are not compensated in real time. The only exception for this is the second order nonlinearity term for the accelerometer. This error source becomes critical if the vibration levels of the sensor changes during the mission. Because of the DC change of sensor output, bias term may be very disturbing. If the second order nonlinearity term is high for the mission, some mechanical solutions or the online vibration measurements may be required to get correct acceleration output.

Bias, scale factor and misalignment parameters of the models are determined and compensated in real time after the sensors are placed on the three axes of the Inertial Measurement Unit. In this way, time and cost can be reduced. For three gyroscopes and accelerometers bias is compensated first, then the scale factor and misalignment corrections can be made as given in Figure 3.

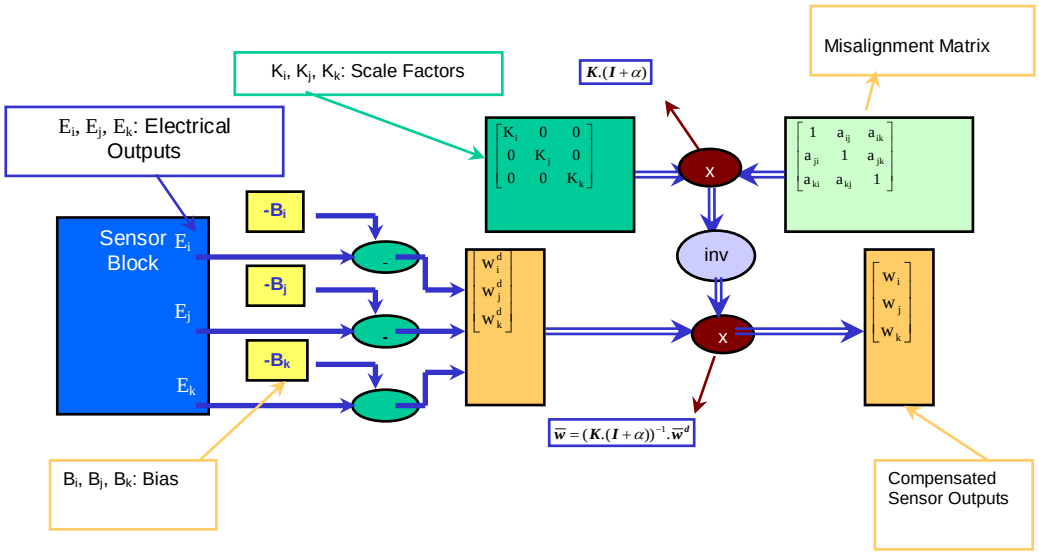

Figure 3: Gyroscope and Accelerometer Model Compensation Technique

After this process it is also possible to compensate the temperature effects and the nonlinearity effects of the sensor, mutually. The model used for each sensor is given in (17) [9]. The main disadvantage of this technique is the necessity of determining the unknown 3x4 coefficient matrix. To do this, one should make quite a number of tests at different stabilized temperature and at different input levels.

$$\omega = \omega_g - \begin{bmatrix} T^2 & T & 1 \end{bmatrix} \begin{bmatrix} c_{00} & c_{01} & c_{02} & c_{03} \\ c_{10} & c_{11} & c_{12} & c_{13} \\ c_{20} & c_{21} & c_{22} & c_{23} \end{bmatrix} \begin{bmatrix} \omega_g^3 \\ \omega_g^2 \\ \omega_g \\ 1 \end{bmatrix} \tag{17}$$

The ω_g term represents the compensated output of an inertial sensor, and T is the temprature.

The processes explained up to this point is for determining and compensating the systematic errors of inertial sensors. After these compensations, the measurement still contains some noise components. These noise components are random drift errors on bias and scale factor uncertainties as given in (18) [3].

$$V = [I + D]\left[1 + 10^{-6}\varepsilon_k\right] \tag{18}$$

Where

V : Output of the Sensor
I : Inertial Input Terms
ε_k : Scale Factor Error (includes scale factor nonlinearity, and asymmetry)
D : Random Drift Rate (includes random walk, bias instability, rate random walk and ramp)

In this thesis, mainly random drift errors, D, will be our concern and in Section 2.2 these error characteristics will be introduced.

3.2 Stochastic Error Models of Inertial Sensors

Main stochastic error sources of inertial sensors are quantization, angle random walk, Gauss-Markov, bias instability, rate random walk and rate ramp noises. All these noises can be generated from a white noise sequence by a rational or non-rational transfer functions, [3]. When variances of these noise sources are examined it can be observed that, quantization, angle random walk and Gauss-Markov noise sources has a constant variances independent of the data length. However, others have variable variances for different data lengths. The reason for this is the non-stationary nature of these noise sources. Therefore if an inertial sensor contains all these noise sources, its output variance changes with data length.

The main acceptation about the stochastic error sources of the inertial sensors is their independency in a probabilistic sense. With this assumption all noise sources can be handled separately. This assumption brings some simplification into the computations. For example variance of the inertial sensor output is evaluated by summing the individual noise source variances.

We can analyze the above mentioned noise sources by analyzing the power spectral density (PSD) of the noise. Note that if the noise under study is the output of a system with a transfer function of the form $(1/s)^m$, where m is an integer (in the continuos time) driven by white noise then it has even powers of the frequency in PSD. The log-log plot generated by using this PSD has a slope which is equal to -2m. Bias instability noise, i.e., 1/f noise, on the other hand has a -1 slope on this plot and since it has the transfer function of $(1/s)^{1/2}$. In some studies the model for this noise is approximated by a Gauss- Markov or multiple stage ARMA model. But these approximations sometimes cause problems if a Gauss-Markov or the other noise sources exist at the sensor output.

Because of the very low frequency nature of the rate ramp noise, it is not included in the stochastic model of the inertial sensor. Low frequency nature implies that its effect can be observed only after a long investigation period of the data. It has a slope of -3 in PSD log-log plot. In other words it can be considered as integral of flicker noise.

In the following subsections well known spectral density functions, Allan variances and white noise driven discrete model of six noise sources of the sensor are given.

3.3 Quantization Noise

Quantization noise is strictly due to the digital nature of the sensor output. The rate PSD and Allan Variance for this noise is given in (19) and (20):

$$S_Q(f) = \frac{4Q^2}{\tau_0}\sin^2(\pi f \tau_0) \tag{19}$$

$$\sigma_Q^2(\tau) = \frac{3Q^2}{\tau^2} \tag{20}$$

Related slope in the square root Allan variance of the log-log plot is –1. The unit of Q is in radians for gyroscopes and m/s for accelerometers.

The power spectral density of the quantization noise has the same characteristics as that of one sample difference of the white noise. This fact is stated in the following lemma.

Lemma 1: Quantization noise can be modeled as the output of the filter $H(z) = (1 - z^{-1})$ driven by white noise.

Proof:
The power spectral density of the quantization noise, given in (19), can be written as

$$\begin{aligned} S_Q(f) &= \frac{4Q^2}{\tau_0}\sin^2(\pi f \tau_0) = \frac{2Q^2}{\tau_0}(1-\cos(2\pi f \tau_0)) \\ &= \frac{Q^2}{\tau_0}\left(2 - e^{j2\pi f\tau_0} + e^{-j2\pi f\tau_0}\right) = \frac{Q^2}{\tau_0}\left[e^{j\pi f\tau_0}\left(1 - e^{-j2\pi f\tau_0}\right)\right]^2 \end{aligned} \tag{21}$$

This spectrum can be obtained from white noise by filtering it with $(1 - z^{-1})$ transfer function.

3.4 Angle Random Walk

Angle random walk is characterized by a white noise on the gyro rate output. The associated PSD is:

$$S_{AR}(f) = (AR)^2 \tag{22}$$

where,

AR is the angle random walk coefficient and its unit is $\text{deg}/\sqrt{\text{sec}}$ (and $m/\sqrt{\text{sec}}$ for accelerometers)
Allan Variance can be obtained as;

$$\sigma_{AR}^2(\tau) = \frac{(AR)^2}{\tau} \tag{23}$$

Therefore the log-log plot of Root Allan Variance has a slope of –1/2. [3]

3.5 Gauss-Markov Noise

Gauss Markov noise is characterized by an exponentially decaying function with a finite correlation time [3]. The first order Gauss-Markov (GM) process in discrete time can be written as [11];

$$x_k = e^{-\frac{\Delta t}{Tc}} x_{k-1} + w_k \tag{24}$$

In this expression Tc is the correlation time of the GM noise. The equation shows that the Gauss-Markov noise can be considered as the output of a first order system driven by white Gaussian noise. The related transfer function is the following one.

$$H_{GM}(z) = \frac{1}{1 - e^{-\frac{\Delta t}{Tc}} z^{-1}} \tag{25}$$

The associated variance is given by [11];

$$\sigma_{x_k}^2 = \frac{\sigma_{w_k}^2}{1 - e^{-\frac{2\Delta t}{Tc}}} \tag{26}$$

Allan Variance of this sequence is given in [3] as;

$$\sigma_{x_k}^2(\tau) = \frac{\left(\sigma_{w_k} T_c\right)^2}{\tau}\left[1 - \frac{T_c}{2\tau}\left(3 - 4e^{-\frac{\tau}{Tc}} + e^{-\frac{2\tau}{Tc}}\right)\right] \tag{27}$$

When τ is much longer than the correlation time it can be approximated as:

$$\sigma_{x_k}^2(\tau) \approx \frac{\left(\sigma_w T_c\right)^2}{\tau} \tag{28}$$

If τ much smaller than the correlation time, then the Allan variance can be approximated as [3];

$$\sigma_{x_k}^2(\tau) \approx \frac{\sigma_w^2}{3}\tau \tag{29}$$

If white noise input of the system has a variance G^2, unit of G is $(\deg/\ hr)/\sqrt{hr}$ for gyroscopes and $\left(m/\sec^2\right)/\sqrt{\sec}$ for accelerometers.

3.6 Bias Instability

The origin of bias instability is the electronics, or other components susceptible to random flickering. Because of its relatively low-frequency nature it shows up as the bias fluctuations in the data. The rate PSD associated with this noise is:

$$S_{BI}(f) = \left(\frac{B^2}{2\pi}\right)\frac{1}{f}\ ;\ f \le f_0 \tag{30}$$

where B is the bias instability coefficient and its unit is deg/sec for gyroscopes and m/sec^2 for accelerometers. f_0 is the cutoff frequency.

Allan Variance can be obtained as [3];

$$\sigma_{BI}^2(\tau) = \left(\frac{B}{0.6648}\right)^2 \tag{31}$$

Therefore the log-log plot of this noise has zero slope [3].

Bias instability noise can be produced as the output of the irrational transfer function given below when the input is white noise.

$$H_{BI}(z) = \frac{1}{(1-z^{-1})^{\frac{1}{2}}} \tag{32}$$

3.7 Rate Random Walk

This is a random process of uncertain origin, possibly a limiting case of an exponentially correlated noise with a very long correlation time. The PSD and Allan Variance associated with this noise are:

$$S_{RRW}(f) = \left(\frac{K}{2\pi}\right)^2 \frac{1}{f^2} \tag{33}$$

$$\sigma^2_{RRW}(\tau) = \left(\frac{K^2}{3}\right)\tau \tag{34}$$

where K is the rate random walk coefficient and its unit is deg/hr/hr^{½} [3] for gyroscopes, m/sec^2/sec^{½} for accelerometers. Root Allan Variance of this noise has +1/2 slope.

Since, rate random walk is the integral of the white noise, the related transfer function can be written as;

$$H_{RRW}(z) = \frac{1}{(1-z^{-1})} \tag{35}$$

3.8 Rate Ramp

For long, but finite time intervals this is more of a deterministic error rather than a random noise. For an Interferometric Fiber optic Gyroscope (IFOG) it is given in time domain as $\Omega = Rt$ where R is the rate ramp coefficient and Ω is the output of IFOG corresponding to rate ramp. Its unit is deg/hr/hr for gyroscopes. By forming and operating on the clusters of data containing an input, we obtain:

$$\sigma^2_{RR}(\tau) = \frac{R^2\tau^2}{2} \tag{36}$$

This indicates that the rate ramp noise has a slope of +1 in the log-log plot of $\sigma(\tau)$ versus τ [3].

3.9 Stochastic Model Used in the Study

Although rate ramp noise is included in the stochastic model of an inertial sensor, it is treated as a deterministic noise source as explained previously. Therefore it is excluded from the model for this study. In fact once it is determined it can be completely compensated like a bias or a scale factor of an inertial sensor.

Very low frequency sinusoidal noise is also included in the stochastic model of the inertial sensor. However, this noise is again excluded from the model used in this study because of the same reason.

Our model for an inertial sensor used in this study contains quantization, angle random walk, Gauss-Markov, bias instability and rate random walk noise sources and is given schematically in Figure 4.

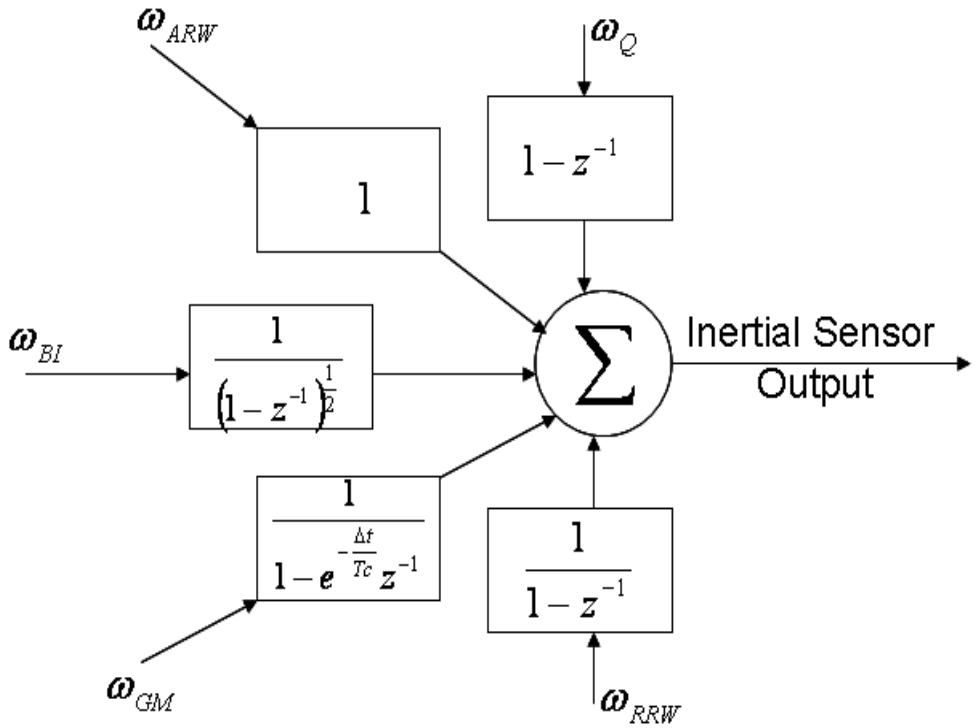

Figure 4: Stochastic Model of Inertial Sensor used in this study

CHAPTER 4

VARIANCES OF DIFFERENCES

Allan variance and the online estimation methods proposed up to now has some advantages and disadvantages in terms of performance and calculation load. For example, Allan variance method can be used to identify all of the stochastic error sources of an inertial sensor. On the other hand, noise sources with small power can not be determined accurately, because of its graphical parameter estimation strategy. High calculation load can be considered as another disadvantage of this method. Online estimation techniques are very good with its reduced calculation load and high performance in the estimation accuracy even for low power noises. However, only a limited number of the noise sources can be modeled and identified and the existence of a noise source that is not modeled will degrade the estimation performance.

The proposed method, whose theory and the algorithm explained in the following sections, is a very powerful method to identify the noise parameters of an inertial sensor. Usage of this method provides high accuracy in the estimation of the noise parameters with a reduced calculation load.

Since bias instability and rate random walk noise sources are non-stationary inertial sensor output including these noise sources is also non-stationary. Therefore, looking at the sensor variance directly does not give any useful information to discriminate and identify the different noise sources. The method suggested in this study uses the differences of original sensor outputs and its delayed versions. This approach is new and one of the contributions of this thesis.

Although the main reason of choosing the differencing technique is the stationarity of the resultant signal it also has interesting properties in the frequency domain. The transfer function of the operation of taking the difference of elements of the given sequence can be modeled the difference waveform as the output of the system with the transfer function $H_L(z) = (1 - z^{-L})$. The magnitude plots of the system are given in Figure 5 for different L values. This filter is a special comb filter. So it selects some frequencies that exist in the signal. This property encourages us to use it to find the power of the different noises that exist in the output of an inertial sensor. As an example when L=1 the filter is a high pass filter so eliminates the low frequency noise like rate random walk and concentrates on the others. On the other hand when L is large almost all noises are effective so it becomes possible to find the power of low frequency noises. Very simple structure of the filter and the partly unknown frequency content of any noise make this filter attractive. Another approach may be using wavelet filters that we suggest as a further study.

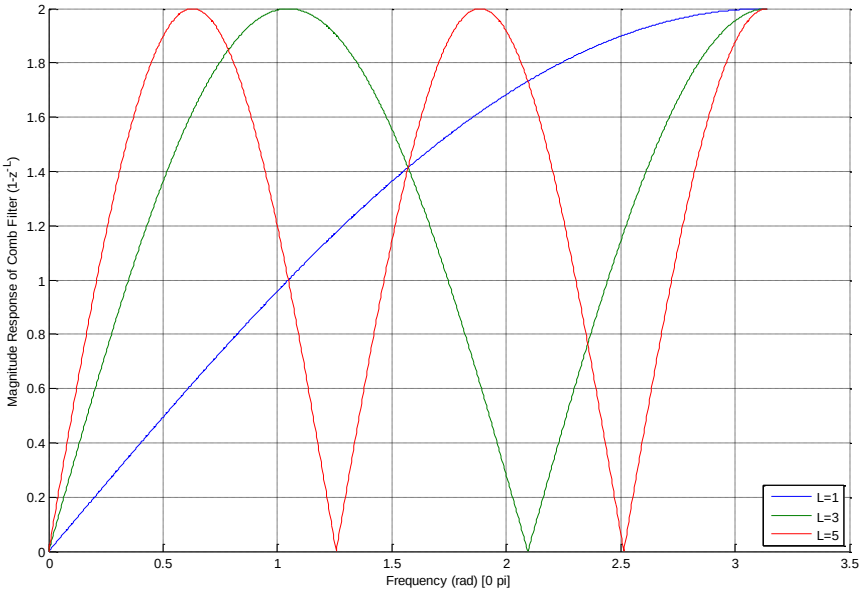

Figure 5: Magnitude response of the comb filter

Variances of difference sequences for the sensor output and each noise source will be given in the following subsections. In all the derivations we assume that the input white noise is zero mean and has the variance σ^2.

4.1 Sensor Output Difference Variance

Inertial sensor output considered in this study is assumed to include quantization, angle random walk, bias instability, rate random walk and correlated Gauss-Markov noise sources. The model can be extended to include rate ramp noise source but we leave it as a future work.

Let the inertial sensor output be $g[n]$. Then referring to Figure 4,

$$g[n] = g_{QN}[n] + g_{AR}[n] + g_{BI}[n] + g_{RR}[n] + g_{GM}[n] \tag{37}$$

where; $g_{QN}[n], g_{AR}[n], g_{BI}[n], g_{RR}[n], g_{GM}[n]$ are quantization, angle random walk, bias instability, rate random walk and Gauss-Markov noises.

K step difference sequence, called $g_{dK}[n]$, is defined as;

$$\begin{aligned} g_{dK}[n] &= g[n] - g[n-K] \\ &= \left(g_{QN}[n] - g_{QN}[n-K]\right) + \left(g_{AR}[n] - g_{AR}[n-K]\right) + \left(g_{BI}[n] - g_{BI}[n-K]\right) \\ &\quad + \left(g_{RR}[n] - g_{RR}[n-K]\right) + \left(g_{GM}[n] - g_{GM}[n-K]\right) \end{aligned} \tag{38}$$

Each difference sequence can be considered as the outputs of some system driven by independent white noise. Therefore, variance of the K step difference of the sensor

output is equal to the sum of the variances of each difference sequence if the sequences are independent. For the formulation to be useful we would like to emphasize the stationarity of these sequences that is shown below.

4.2 Difference Variance of Quantization Noise

Quantization noise can be obtained from white noise by filtering it with the transfer function
$H(z) = (1 - z^{-1})$. This noise is wide sense stationary with zero mean and variance $2\sigma^2$ where σ^2 is the variance of the white noise. Transfer function of the combined system difference of quantization noise and its delayed versions can be obtained as given by,

$$H_d(z) = H(z) - z^{-K}H(z) = H(z)\left(1 - z^{-K}\right) \tag{39}$$

The time domain expression is $g_{QN}[n] = (w[n] - w[n-1]) - (w[n-K] - w[n-1-K])$. From the expression the output variances can be obtained as follows.

$$\sigma_Q^2 \cong \begin{array}{l} 6\sigma^2 \text{ for K} = 1 \\ 4\sigma^2 \text{ for K} \rangle 2 \end{array} \tag{40}$$

Note that a sequence obtained by filtering the white noise with $H_d(z)$ is stationary.

4.3 Difference Variance of Angle Random Walk Noise

Angle Random Walk noise of an inertial sensor is white noise. Therefore, its difference variance σ_{ARW}^2 is always equal to the two times the input white noise variance.

4.4 Difference Variance of Gauss-Markov Noise

Let x_k be a GM noise sequence generated by the following equation.

$$x_k = e^{-\frac{\Delta t}{Tc}} x_{k-1} + w_k \tag{41}$$

Where, Δt is the sampling rate, $\mathrm{T}c$ is the correlation time and w_k is IID white noise which is zero mean and variance σ^2. Steady state variance of the sequence x_k is equal to;

$$\sigma_{x_k}^2 = \frac{\sigma_{w_k}^2}{1 - e^{-\frac{2\Delta t}{Tc}}} \tag{42}$$

In order to find the variance of the difference signal of this sequence, it is assumed that the length of sequence is much bigger than the difference so that variances of x_k and x_{k-n} are equal, i.e., the sequence is at the steady state.

$$\mathrm{var}(x_k - x_{k-n}) = E\left\{(x_k - x_{k-n})^T (x_k - x_{k-n})\right\} = 2\,\mathrm{var}(x_k) - 2E\left\{x_k x_{k-n}^T\right\} \tag{43}$$

Since,

$$E\left\{x_k x_{k-n}^T\right\} = e^{-\frac{n\Delta t}{Tc}}\,\mathrm{var}(x_k) \tag{44}$$

then;

$$\mathrm{var}(x_k - x_{k-n}) = \frac{2\sigma_{w_k}^2 (1 - e^{-\frac{n\Delta t}{Tc}})}{1 - e^{-\frac{2\Delta t}{Tc}}} \tag{45}$$

Difference variances for GM noise for 3 sec correlation time are normalized with the input noise variance and are plotted with respect to the difference interval length in Figure 6. For large difference values the correlation $E\left\{x_k x_{k-n}^T\right\}$ goes to zero with an exponential rate so the normalized variance.

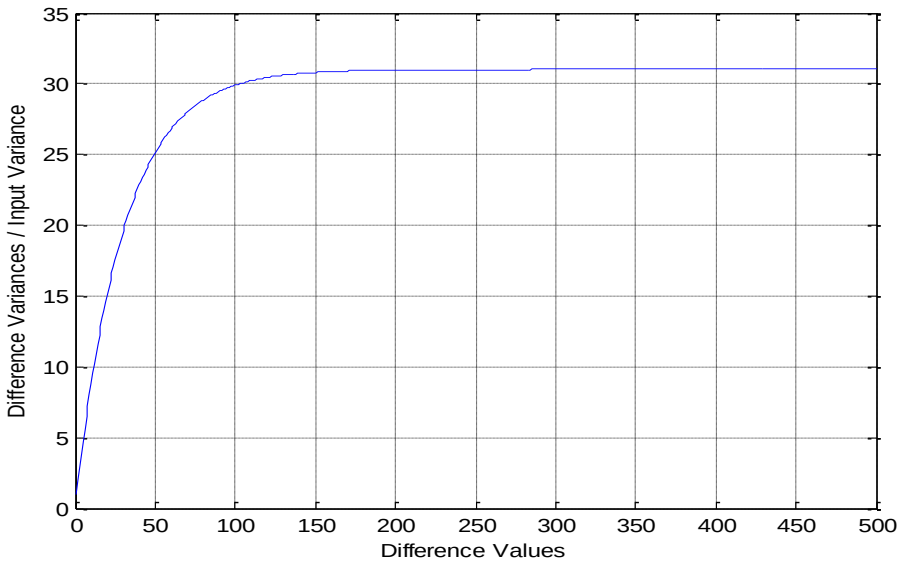

Figure 6: GM noise difference variances (Tc=3sec) normalized with input variance for 0.1sec sampling time

4.5 Difference Variance of Bias Instability Noise

Difference sequence of bias instability transfer function can be written in the same way as the quantization noise by defining the system that generates the difference sequence.

$$H_d(z) = H(z) - z^{-K}H(z) = H(z)\left(1 - z^{-K}\right) \tag{46}$$

Where;

$$H(z) = \frac{1}{(1 - z^{-1})^{\frac{1}{2}}} \tag{47}$$

Approximate infinite impulse response model parameters for the non-rational transfer function of $H(z)$ can be obtained as given in [6];

$$h_0 = 1$$
$$h_k = (k - \frac{1}{2})\frac{h_{k-1}}{k} \quad k = 1,2,... \tag{48}$$

Table II shows the results of the computation of the normalized variances of the difference sequences of the output of this filter up to K=10 where K is the length of the difference interval.

Table II: Normalized variances for first 10 differences intervals of the flicker noise.

K	1	2	3	4	5	6	7	8	9	10
dv/ σ^2	1.2732	1.6977	1.9523	2.1342	2.2757	2.3914	2.4894	2.5742	2.6491	2.7161

Difference variances for bias instability noise are normalized with the input noise variance and are plotted versus difference values in Figure 7. (dv) is for the difference variance.

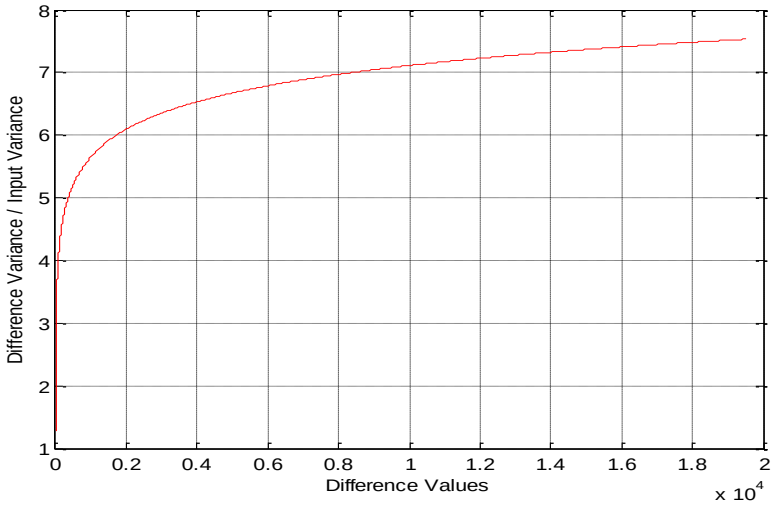

Figure 7: Bias instability noise difference variances normalized with input variance for 1sec sampling time

To apply the method proposed here we need stationary sequences after a transition period. This requirement is satisfied if the system that generates the sequence is stable. The theorem given below guarantees the stability of the system.

Theorem: The difference sequence obtained from Bias instability noise is stationary, i.e., every sequence obtained by filtering the white noise with $H_d(z)$ is stationary.

Proof: From the impulse response model used for bias instability the variance for each difference can be obtained as;

$$Var\{x_k - x_{k-n}\} = \left(h_0^2 + h_1^2 + \ldots + h_{n-1}^2 + (h_0 - h_n)^2 + (h_1 - h_{n+1})^2 + (h_2 - h_{n-2})^2 \ldots\right)\sigma^2 \tag{49}$$

where, x_k is the bias instability noise. Since $h_0^2 + h_1^2 + \ldots + h_{n-1}^2$ is a finite value it must be proved that $\sum_{k=0}^{\infty}(h_k - h_{n+k})^2$ is finite for all *n*. Using (48) we can write:

$$\begin{aligned}
(h_k - h_{n+k})^2 &= \left(h_k - \left(n+k-\frac{1}{2}\right)\frac{h_{n+k-1}}{n+k}\right)^2 \\
&= \left(h_k - \left(n+k-1-\frac{1}{2}\right)\left(n+k-\frac{1}{2}\right)\frac{h_{n+k-2}}{(n+k)(n+k-1)}\right)^2 \\
&= \left(1 - \frac{\left(n+k-\frac{1}{2}\right)\left(n+k-1-\frac{1}{2}\right)\ldots\left(k+1-\frac{1}{2}\right)}{(n+k)(n+k-1)\ldots(k+1)}\right)^2 h_k^2
\end{aligned} \tag{50}$$

Note that n is finite and from (48), $h_k^2 < 1$. The numerator and the denominator of the expression inside the parenthesis are monic polynomials of k and the resultant rational function's numerator degree is one less than the degree of its denominator. This guarantees the convergence of the series $\sum_{k=0}^{\infty}(h_k - h_{n-k})^2$.

Note that the original system with the transfer function $H(z) = \frac{1}{(1-z^{-1})^{\frac{1}{2}}}$ is certainly not stable. So differencing operation is necessary to obtain its unknown parameters.

4.6 Difference Variance of the Rate Random Walk Noise

Rate Random Walk noise of an inertial sensor is the integral of white noise. Therefore, for K=1 difference variance σ_R^2 is equal to the input white noise variance. For K=2, the difference sequence becomes the difference of two independent random variables so its variance is equal to two times the input variance. For the general case consider $x_k = x_{k-1} + \omega_k$ where x_k is the rate random walk and ω_k is a zero mean white noise with variance σ^2. The variance of $x_k - x_{k-n}$ can be obtained as; $x_k - x_{k-n} = \sum_{i=0}^{n-1}(x_{k-i} - x_{k-i-1}) = \sum_{i=0}^{n-1} w_{i-1}$ which is $n\sigma^2$.

Note that this system is also not stable as the system that generates the bias instability noise since it is a simple adder (integrator). Differencing makes the resultant system stable and allows the application of the identification method.

In this section all noises that we assume to exist at the output of an inertial sensor are modeled. Furthermore their differences are also modeled and the steady state variances of them are found. Our ultimate aim is to identify the powers of these signals as well as the correlation coefficient of the GM noise.

CHAPTER 5

LEAST SQUARES ESTIMATION FORMULATION

The main purpose of this study is the identification of the white noise variances that generate the inertial sensor stochastic errors. For this purpose we use the models mentioned in the previous chapter that reduces the problem to a simple identification of noise variances process that can be solved by using the least squares estimation method. The only noise source that requires the identification of a parameter other then input noise variance is GM noise. First assume that the GM noise parameter $\frac{\Delta t}{Tc}$ is known.

$$\begin{aligned} \mathrm{var}(g_{dn}) &= \sigma_Q^2 + \sigma_A^2 + \sigma_B^2 + \sigma_R^2 + \sigma_{GM}^2 \\ &= q(n)\mathrm{Q}^2 + 2A^2 + bi(n)B^2 + nR^2 + gm(n)G^2 \end{aligned} \tag{51}$$

where, $\mathrm{Q}^2, A^2, \mathrm{B}^2, \mathrm{R}^2, \mathrm{G}^2$ are variances of white noise that generate quantization, angle random walk, bias instability, rate random walk and Gauss-Markov noises, respectively. The functions $bi(n)$, $gm(n)$ and $q(n)$ can be obtained as follows;

$$\begin{aligned} bi(n) &= \left(h_0^2 + h_1^2 + \ldots + h_{n-1}^2 + \left(h_0 - h_n\right)^2 + \left(h_1 - h_{n+1}\right)^2 + \left(h_2 - h_{n-2}\right)^2 \ldots\right) \\ gm(n) &= \frac{2(1 - e^{-\frac{n\Delta t}{Tc}})}{1 - e^{-\frac{2\Delta t}{Tc}}} \\ q(n) &= \begin{cases} 6 & \text{for } n = 1 \\ 4 & \text{otherwise.} \end{cases} \end{aligned} \tag{52}$$

In the above formulation n, indicates that to compute the difference we skip exactly ‘n’ samples, i.e., an ‘n difference’ operation is applied to $\{g_i\}$ sequence. The set of differencing interval lengths ‘n’ should be smaller than a fraction of the data length but does not need to include all integers. Indeed the selection of ‘good n’ values is one of the important issues of this method. This problem will be addressed later.

To explain the equations that are solved in the least square sense we give an example of correlation coefficient $Tc = 3\mathrm{sec}.$. The equations for this case can be written as follows.

$$\mathrm{var}(g_{d1}) = \sigma_Q^2 + \sigma_A^2 + \sigma_B^2 + \sigma_R^2 + \sigma_{GM}^2 = 6\mathrm{Q}^2 + 2A^2 + 1.2732B^2 + R^2 + \frac{2(1-e^{-\frac{1}{3}})}{1-e^{-\frac{2}{3}}}G^2$$

$$\mathrm{var}(g_{d2}) = \sigma_Q^2 + \sigma_A^2 + \sigma_B^2 + \sigma_R^2 + \sigma_{GM}^2 = 4\mathrm{Q}^2 + 2A^2 + 1.6977B^2 + 2R^2 + \frac{2(1-e^{-\frac{2}{3}})}{1-e^{-\frac{2}{3}}}G^2$$

$\vdots$

The above equations can be written in the matrix form as:

$$\begin{bmatrix} 6 & 2 & 1.2732 & 1 & 1.1651 \\ 4 & 2 & 1.6977 & 2 & 2.0000 \\ \dots & \dots & \dots & \dots & \dots \\ 4 & 2 & bi[n] & n & gm[n] \end{bmatrix} \begin{bmatrix} Q^2 \\ A^2 \\ B^2 \\ R^2 \\ G^2 \end{bmatrix} = \begin{bmatrix} \mathrm{var}(g_{d1}) \\ \mathrm{var}(g_{d2}) \\ \dots \\ \mathrm{var}(g_{dn}) \end{bmatrix}$$

The functions of the last row of the coefficient matrix are given in (52). The equation is in the form $A_n\xi = G_n$ and the objective function that must be minimized is $\|A_n\xi - G_n\|^2$. The LSE method minimizes the norm $\|A(Tc)X - B\|^2$ where the elements of the A matrix are the difference variances of the individual noise sources given by the theory. The elements of the vector B are obtained by computing the difference variances of the signal for the delay times same as the ones used in the matrix A. A is a function of the time constant, Tc, of the GM correlation function.

In order to characterize the GM noise two parameters namely, the input white noise variance and the correlation time are required. Determination of the input white noise variance is very similar to other stochastic model parameters. On the other hand, the computation of the optimal Tc is unfortunately not very easy due to a highly complicated dependence of the objective function to this parameter. Since the value of the parameter is bounded we have used an extensive search in our experiments to find its value. We have selected the interval as 2-102 sec. with 0.1 sec. increments.

To give an idea about the dependence of the value of the objective function we evaluated it for the input noise parameters given in Table III and plotted with respect to the correlation time in Figure 8. Note that this function is neither convex nor unimodal. Therefore it is difficult to estimate the correlation time using a gradient based optimization algorithm unless a good initial estimate of correlation time known.

Table III: Input noise parameters

Parameters	Q^2	A^2	B^2	R^2	G^2
Input Noise Variances	0.01	0.033	0.0036	0.00028	0.033 (Tc=60, 50, 40, 30, 20,10 sec)

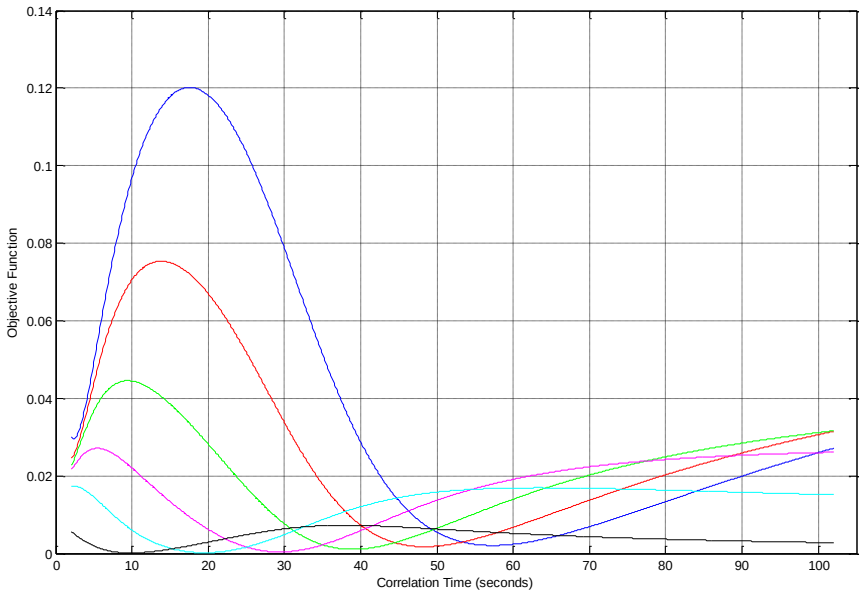

Figure 8: Objective function versus the correlation time

5.1 Selection of the Sequence of Delay Times

Difference variances can be evaluated for every delay time 'n'. Such an exhaustive approach causes a very long evaluation time. Also there may be some problems when using all consecutive delay times since due to the close values in the difference variances (repetition of the data). In order to overcome this problem variable difference interval lengths should be selected with some care. Moreover small difference intervals occur more in their number that causes biased importance towards the high frequency noises. The sequence of differencing lengths chosen must provide both good discrimination of the high frequency noises and a good estimation of the low frequency noise powers.

There are some critical issues in the determination of the delay sequence 'n'. The differencing operation as explained before corresponds to the application of a comb filter to the data. In order to capture the low frequency noise it is required to cover the low frequency bands by the comb filter. That is achieved by using long difference intervals. As an overall result: the first difference is very important for the discrimination of the quantization and the angle random walk noise parameters. Small 'n' values are good for the determination of ARW and GM noise sources with low correlation times. In order to determine RRW and BI noise parameters and also GM noise that has high correlation times high 'n' values are required.

Depending on the data length unexpected variances can be obtained for high difference values because of the insufficient number of data. A method in determination of the difference values that can be used in the proposed algorithm for 10 Hz sensor output is given step by step as follows:

- Use the first 400 delays (k=1,2, …400),
- Evaluate increment size by using the equation; $inc\_size = \frac{1}{60}\frac{data\_length - 400}{40}$,
- Count is equal to 1;
- Starting value of the next delay is *nd*=400+*inc_size***count*. Choose the next 10 delay values as: (k=*nd*, *nd*+1,…,*nd*+9)*;*
- Increase the count by one, until it reaches to 60 and execute the previous step.

We cannot say that the selection of these sequences is optimum for all types of inertial sensor outputs. On the other hand, in the simulations it works quite well for the chosen stochastic model parameters.

The selection of the difference intervals should clearly depend on the data length. A second approach that we have used assumes that the number of intervals is restricted to a given number. Figure 9 assumes that this number is 1000. Our previous experience on the subject shows that one step and two step increases in the difference interval lengths are extremely important in the identification of the high frequency noise. So 300 out of 1000 of the variance data is generated with an increase of one in the difference interval length and 100 out of 1000 with an increase of two. For the remaining 600 interval lengths we have applied a strategy of changing them with much larger steps. To explain the strategy let M be the data length. (M/37.5) corresponds to the largest difference interval. As an example if M=180000 which is the smallest data length given in Figure 9 this number is 4800. The remaining interval lengths will start from 300+2x100=500 and go to 4800 and there are 600 of them. Due to the noisy behavior of the solution we decided to use some clusters for the interval lengths instead of a single value. The cluster length is selected as 30. So each interval length cluster starts from a value say 'k' and increases one by one to 'k+30'. The number of clusters is therefore is 600/30=20. The jump amounts in the interval lengths is assumed to be constant and is calculated as 4800/20. According to this procedure the example data generates the interval lengths as:

Interval length: 1, 2, …, 300, 302, 304, …, 500, 741, 742, …, 770, 981, 982, …, 1010, 1221, 1222, …

The algorithm is given below.

- First 300 interval lengths change from 1 to 300 and increase with one step.
- Interval lengths of 301 to 400 changes from 302 to 500 and increase with 2 steps.
- X=datalength/37.5: largest interval length
- X/20: amount of jump in the interval lengths
- Set increment to zero.
- Interval lengths of (401+30*increment) to (430+30*increment) starts from (increment*(X/20)+500) and increase with one step.
- Increase the increment and repeat the previous step until increment is equal to 21.

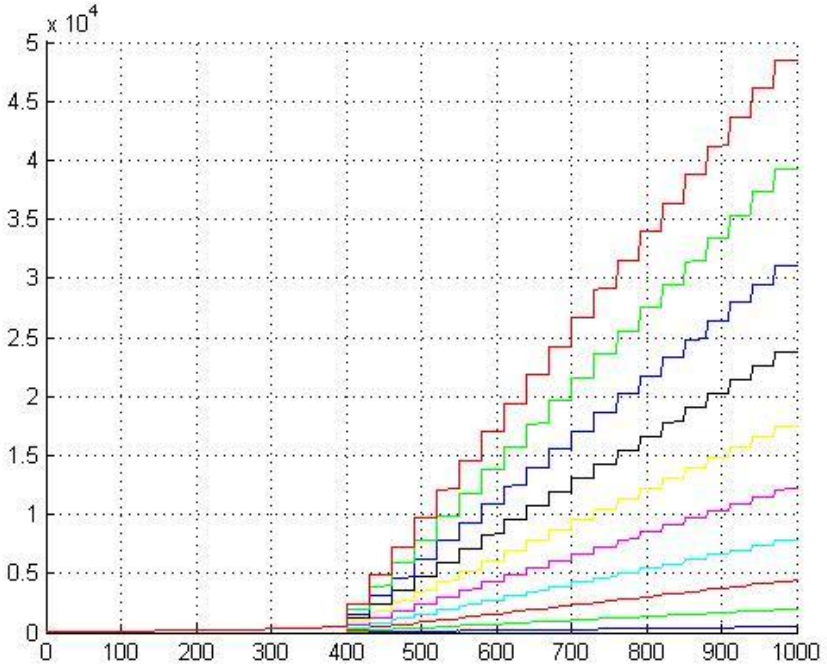

Figure 9: Difference values for different data lengths

The performance of the system highly depends on the strategy of selection of the interval lengths. We applied different strategies to see the effects of using different interval lengths. One of the strategies is to use an appropriate quadratic function in the interval length determination. In this strategy a difference sequence is generated by using the square of the numbers from 1 to 100 incremented by one and the square of the numbers from 100 to 500 incremented by 0,5. The interval lengths are given by the numbers computed. In this strategy we didn't use the concept of clusters.

A third strategy is to use Fibonacci numbers as the interval lengths. The idea of using clusters is also not used in this algorithm. Furthermore the number of interval lengths is quite small which is around 20 compared to 1000 for this algorithm as can be seen from the Figure 10. Figure 10 is plotted for an approximate maximum difference length of 250000. This figure is generated by using approximately the same parameters, except step increase in the first method, used in the simulations given in this study. The step increase used in the first method in the simulations is ¼th of the one given here. The reason for it is to make the visual comparison more clear. As the figure indicates we have selected a very diverse set of algorithms to estimate the unknown parameters. At this step we can say that the worst performing algorithm is Fibonacci as can be expected and the best one is the 'stepwise increase'. More detailed conclusions are given at the end of the related experiments. Note that all three algorithms use increasing sequence of degree at least two as the interval lengths.

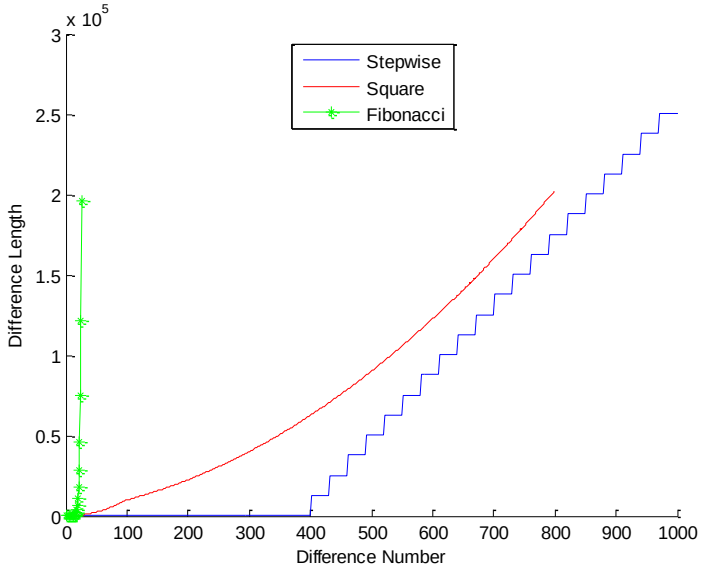

Figure 10: Difference lengths generated by different strategies

5.2 Sampling Time

The algorithm up to now is explained for a sampling time of one second. However, the sampling time for tactical grade navigation system is 0.01 second or less than this. It is possible to obtain lower sampling frequency output by combining samples of the inertial sensor. This causes a low pass effect on the data. As a result of such a process determination of high frequency quantization noise parameter is badly effected as expected. Our experiment shows us that 0.1 Second sampling time is quite good to determine this parameter. The proposed algorithm requires some modifications if the sampling rate is different than one second.

Quantization noise variance is inversely proportional to sampling time. Angle random walk or white noise variance does not depend on sampling time. Bias instability variance is proportional to square root of the sampling time, Gauss-Markov and rate random walk noise variances are proportional to the sampling time. Therefore, first column of the predefined A matrix must be divided by the sampling time, second column remains unchanged, third column of it must be multiplied by the square root of sampling time, fourth and fifth columns of the matrix are multiplied by the sampling time. After the modifications when the sampling time is ST the equation takes the following form.

$$\begin{bmatrix} \frac{6}{ST} & 2 & \mathbf{1.2732}\times\sqrt{ST} & 1\times ST & 1.1651\times ST \\ \frac{4}{ST} & 2 & \mathbf{1.6977}\times\sqrt{ST} & 2\times ST & 2.0000\times ST \\ \dots & \dots & \dots & \dots & \dots \\ \frac{4}{ST} & 2 & bi[n]\times\sqrt{ST} & n\times ST & gm[n]\times ST \end{bmatrix} \begin{bmatrix} Q^2 \\ A^2 \\ B^2 \\ R^2 \\ G^2 \end{bmatrix} = \begin{bmatrix} \mathrm{var}(g_{d1}) \\ \mathrm{var}(g_{d2}) \\ \dots \\ \mathrm{var}(g_{dn}) \end{bmatrix}$$

Effect of total simulation time is important especially for the computation of low frequency noise sources, namely bias instability and rate random walk noise parameters. This requirement is enhanced further because of the very low input noise power.

5.3 Weighted Least Squares Estimate

Difference variances are obtained from the original sequence and its delayed versions. In order to evaluate the K^{th} difference of the data with dimension L; the data from 1 to L-K is differentiated from the data from K+1 to L. Therefore the effect of non-stationarity becomes important if difference value is big as compared to L.

Especially for BI and RRW noises, increase in difference interval causes high difference variance error because of their non-stationary characteristics and finite data length. In order to analyze this effect for these two noise sources, difference noise variances are calculated for the generated data with 0.1 sampling time and unit input variance and compared with the expected noise variances. Increasing the data length reduces the error however cannot remove this effect completely.

For BI noise, approximately 10 and 50 hours simulated data is used. The error between the expected and evaluated noise variance versus difference variances is plotted in Figure 11.

Increase of the data length from 10 hours to 50 hours reduces the error however can not remove it completely. Note that up to difference interval lengths of 4000, error is acceptable for both data lengths. On the other hand for higher difference values error becomes unacceptable due to the non stationary character of the data. Note that the comparison of the two figures shows this effect of non stationarity clearly.

Similarly, for RRW noise approximately 10 and 50 hours simulated data is used and the error between the expected and evaluated noise variance versus difference interval lengths is plotted in Figure 13.

The experiments are repeated 10 times. As a result of these Monte Carlo runs the obtained average errors are plotted for both BI and RRW noise sources. Figure 12 for BI noise and Figure 14 for RRW noise show that the increase in simulation time decreases the average error.

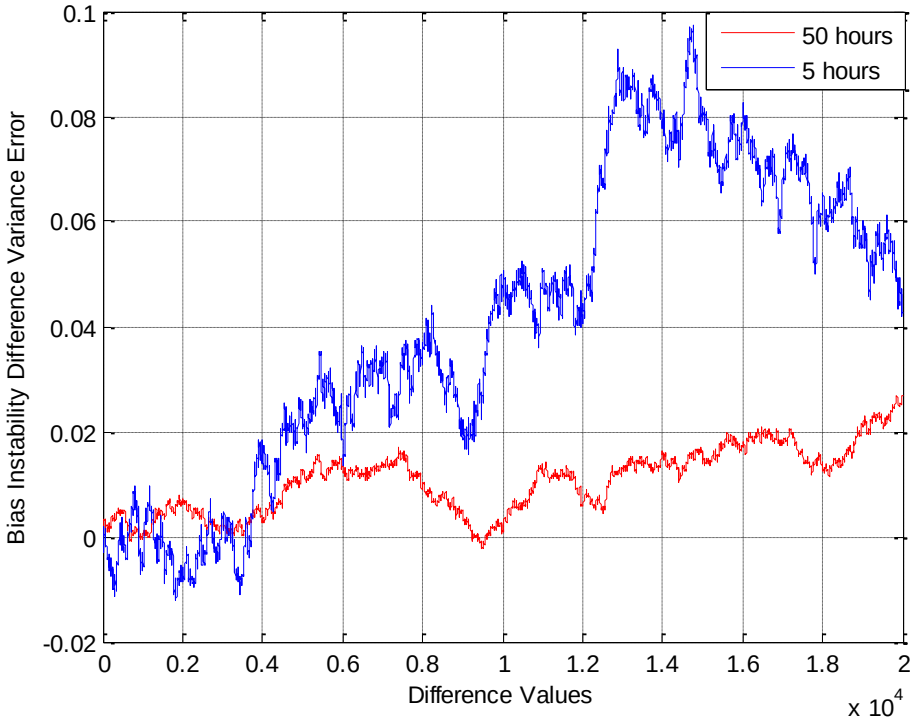

Figure 11: BI noise difference variance errors (Blue: 50 hours, Red: 5 hours)

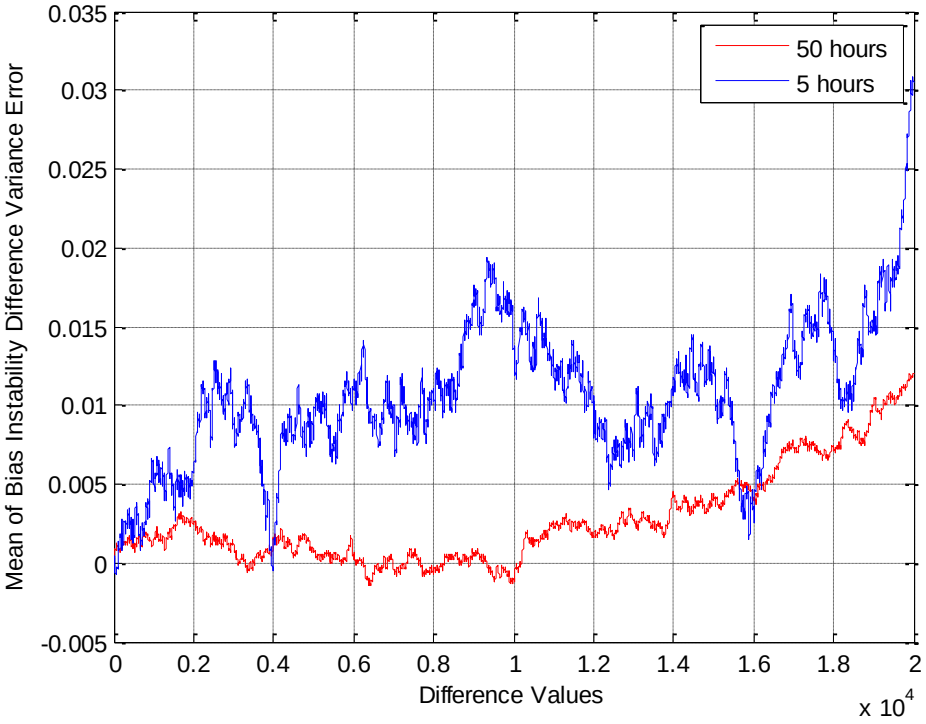

Figure 12: Average error of BI difference variance

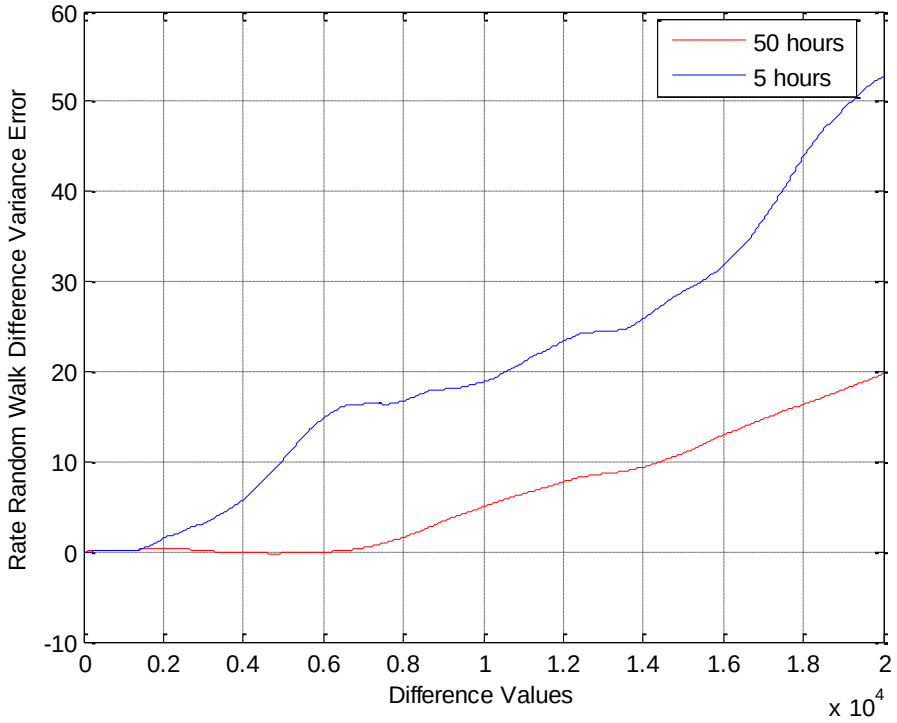

Figure 13: RRW noise difference variance errors (Blue: 50 hours, Red: 5 hours)

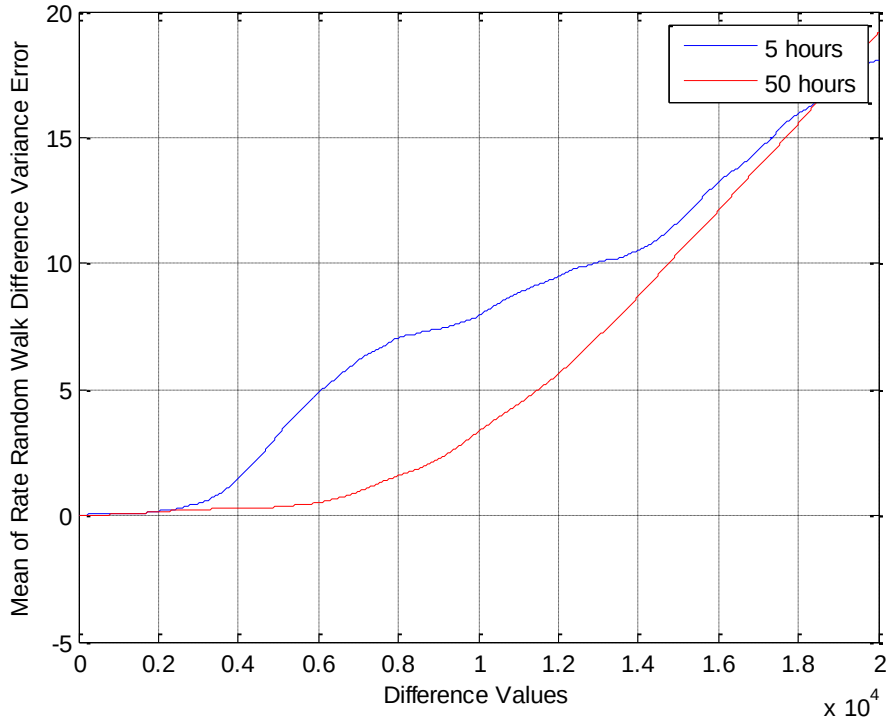

Figure 14: Average error of RRW difference variance

For the RRW noise, error in difference variances increases as the interval length increases for both data lengths. For difference interval length of up to 4000, error in difference variances are relatively small but even for this interval, unlike the BI noise, they are not suitable to be used in the algorithm directly. The error plots given in Figure 11 Figure 14 are the errors corresponding to input noises of power 1, i.e., they are normalized with the input variance. Input variance for the BI is around 0.1 and RRW is 0.001 for tactical grade inertial sensors. So the absolute errors are in the order of 10^{-3} for both of the sensors.

The degradation in the performance as interval length increases is not observed for the other noise sources. Their plots are given in Figure 15, Figure 16 and Figure 17. Increase in data length reduces the error, but the error is independent from the difference values. We believe that this is due to the stationary character of this noise.

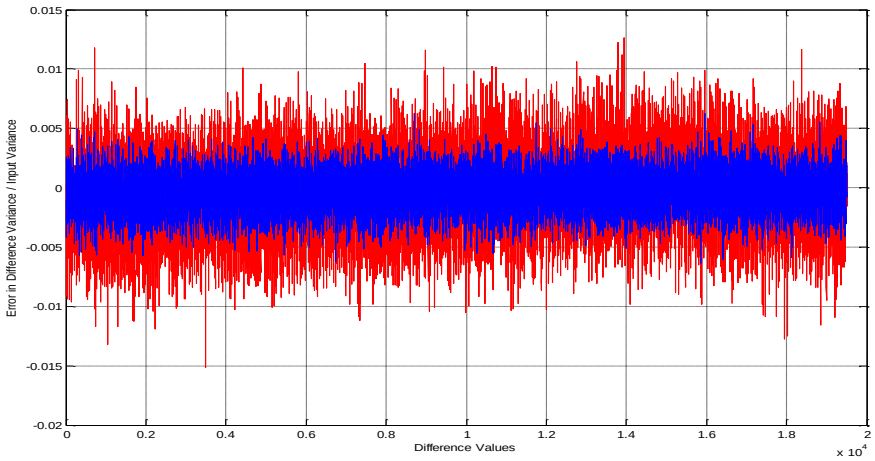

Figure 15: ARW noise difference variance versus error difference values (Blue: 50 hours, Red: 5 hours)

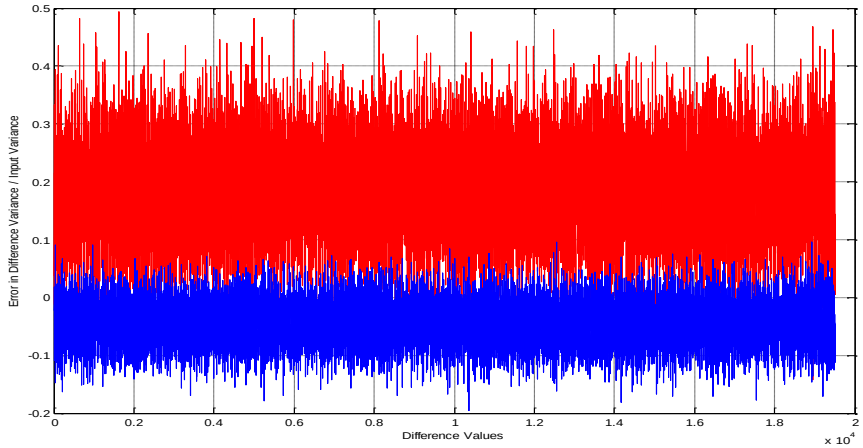

Figure 16: QN noise difference variance versus error difference values (Blue: 50 hours, Red: 5 hours)

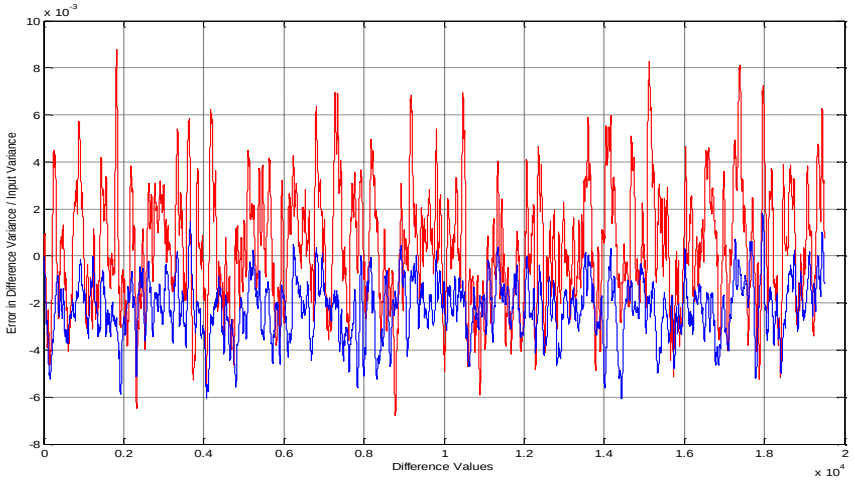

Figure 17: GM noise difference variance versus error difference values (Blue: 50 hours, Red: 5 hours)

As indicated above the difference variances for the sensor outputs containing BI and RRW noise sources evaluated becomes unreliable for difference interval lengths greater than 4000 for the 0.1 sec sampling time. We said that the reason for it is the non stationary nature of these noises. These noises contain low frequency fluctuations which are not stable. Differencing is unavoidable for the computation of their input powers. Even after this operation they require long interval lengths for the reliable computation of their parameters. Since the data length is limited even for 50 hours case, as the interval length increases it becomes in sufficient due to the reason that at the very beginning and the end of the data creates a non-stationarity. The situation is explained in Figure 18. In the figure we assume that the length of data is N and the length of the interval is N/3. The middle part of the data i.e., 1/3rd of it is used two times in the computation of the interval variances while the 1/3rd at the beginning and 1/3rd at the end are only used once. This causes some kind of non-stationarity in the computations.

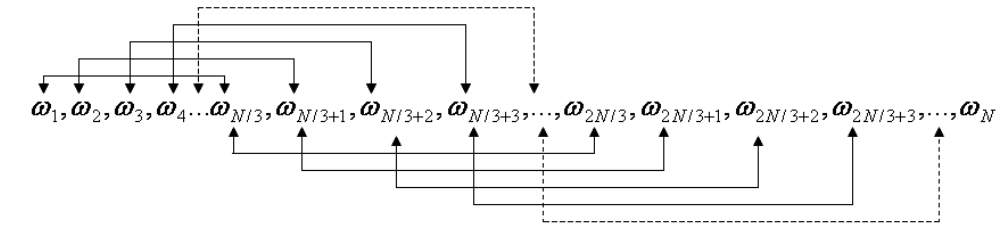

$$g^1 = \omega_1, \omega_2, \omega_3, \omega_4 \ldots \omega_{N/3}, \omega_{N/3+1}, \omega_{N/3+2}, \omega_{N/3+3}, \ldots, \omega_{2N/3}$$

$$g^2 = \omega_{N/3+1}, \omega_{N/3+2}, \omega_{N/3+3}, \ldots, \omega_{2N/3}, \omega_{2N/3+1}, \omega_{2N/3+2}, \omega_{2N/3+3}, \ldots, \omega_N$$

Common Data For Both Sequence for N/3 difference value

$$DifferenceVariance \overset{\Delta}{=} \mathrm{var}(g^1 - g^2)$$

Figure 18: Calculation of difference variances

The requirement of long difference intervals and the requirement of stationarity are conflicting. The conflict is tried to be solved by using a weighting matrix. Using a weighting matrix to reduce the reliability to high difference values usually give better result for the estimation as expected. Depending on the nature of the data a suitable weighting function can be determined. Very low weighting values for high intervals may cause the poor estimation of low frequency noise parameters. Weighting function used for the simulations is selected as $0.9999^{difference\_value}$. Increasing this number results in high convergence rate for the parameters, but causes instabilities especially for limited data.

CHAPTER 6

SIMULATIONS AND RESULTS

Allan Variance is one of the best methods to identify the stochastic model parameters of the inertial sensors. Therefore we have generated artificial data with known noise parameters and estimate the known parameters both using Allan variance method and our method and compare the results. In order to generate bias instability noises, Auto Regressive (AR) model is used as suggested in [6]. Delay times are selected as the first 27 Fibonacci numbers. The results are given in Table IV and the Allan variance plot is given in Figure 19.

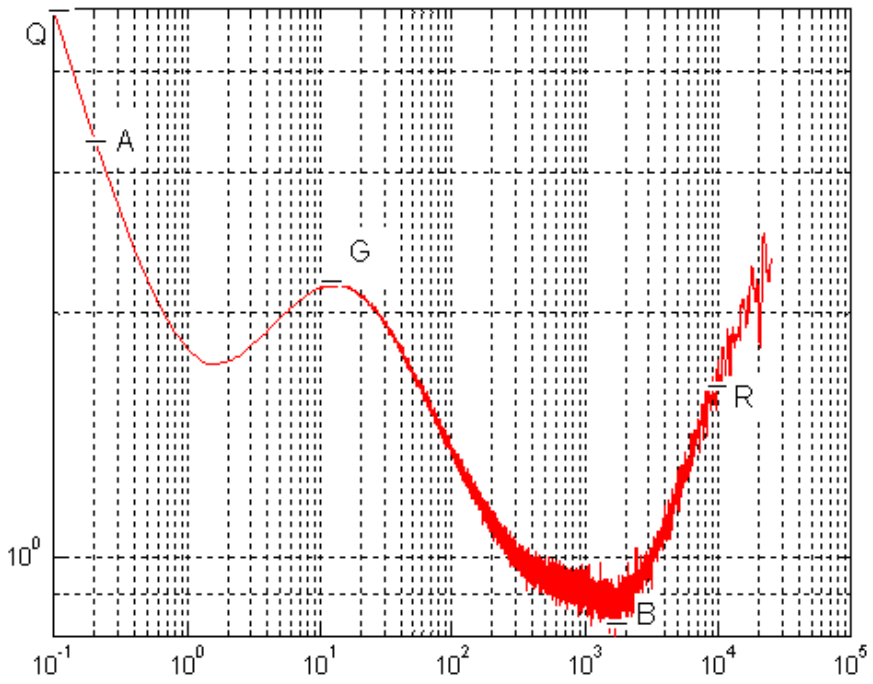

Figure 19: Allan variance plot of the first example

Table IV: Comparison of the Allan variance method and the proposed method

Parameters	True Values	Values computed by Allan Variance	Values computed by the proposed method
Q^2	0.01	0.0076 (at t=0.1s)	0.0102
A^2	1.9	2.197 (at t=0.2 s)	1.8950
B^2	1	1.4559(at t=1661.6 s)	1.0292
R^2	0.0005	0.00083 (at t=10000s)	0.000323
G^2	3 (7 sec Tc)	3.6486 (6.825 s Tc)	2.9907 (7.01 sec Tc)

Results obtained from the proposed method are much better than the results of the Allan variance method even we used the Fibonacci selection which uses only 27 equations in this simulation. When multiple error sources exist, Allan variance method is successful if the different noise terms appear in different regions of cluster time. This example indicates that our method is more robust to variations in the multiple error sources which is the main advantage of the proposed method over Allan variance. The conclusion here is also supported by other simulation examples as well as the one using the real data.

Since all of the predefined stochastic noise error models used in this study can be characterized according to its variance and the sampling rate, except for the GM noise, the performance of the algorithm must be evaluated for different GM correlation times and for different data lengths. For this purpose, input variance parameters given in Table V are used. Correlation times of the GM noises are changed from 3 sec to 21 sec by 2sec steps. Allan variances of the selected case are given in Figure 20 and the percentage errors for the noise parameters are given in Figure 21 for different input sequence lengths. Sampling time is taken as 0.1 sec for all simulations and difference lengths are chosen as Fibonacci numbers. Percentage error is defined as;

$$percentage\_error = 100 \times \frac{|true\ value - estimated\ value|}{true\ value}$$

.

Table V True values of the noise parameters used in the simulation

Parameters	A^2	B^2	R^2	Q^2	G^2
Input Noise Variances	1.9	0.7	0.005	0.5	0.6

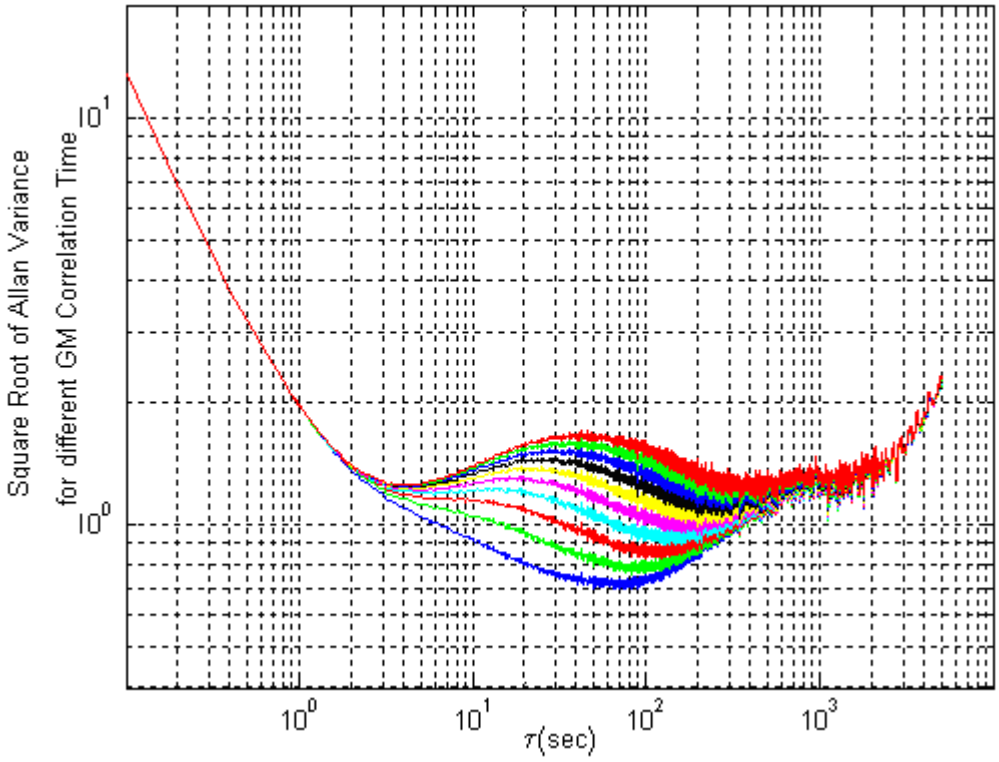

Figure 20: Allan variance plot for different GM correlation times. Increasing curves correspond to increase in correlation times from 3sec to 21sec by 2sec steps

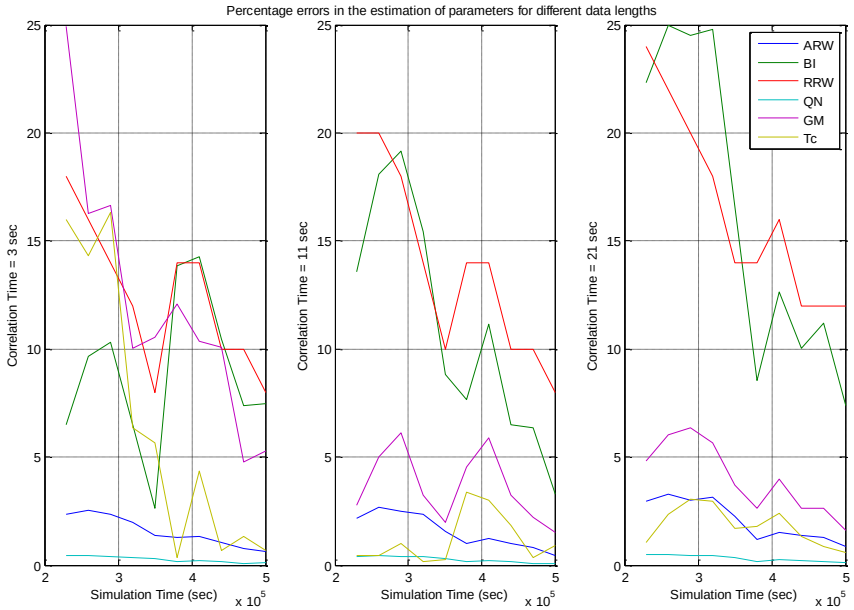

Figure 21: Percentage errors in the estimation of parameters for different simulation times

Generally, the performance of the algorithm increases by increasing the data length as shown in Figure 21. Increase in the correlation time of the GM noise reduces the estimation accuracy of bias instability and rate random walk noise variances. The increase in the errors of the parameters of BI and RRW noises is due to the wrong weight selection for the data lengths for around 110 hours. That observation implies that the selection of the weighting function should be further optimized according to the interval length selection strategy (Fibonacci for this experiment) and the data length. That is one of the future work that we propose.

Figure 22 shows the difference variances of different noise sources with respect to the difference interval length. As the figure shows it is not possible to differentiate low pass noise sources, RRW, BI furthermore GM (with high correlation times) noise shows similar character when the difference interval lengths are small as indicated in (C) and (D) part of the figure. For such a situation estimation of the input powers of the noise sources cannot be differentiated by the proposed Least Squares Estimate algorithm. The quantization noise and angle random walk noise parameter estimation performance remains almost unchanged for different correlation times of the GM noise. This result can be explained again by examining Figure 22 as the figure indicates that the characteristics of the noise sources are different for other 3 noise sources for any differentiation interval length. Estimation accuracy of GM noise parameters, the noise variance and the correlation time, is much better for high correlation times. In fact, the absolute error in the estimation of the correlation times is almost same but percentage errors become small for high correlation times. When the results are examined, it is observed that, the performance of the algorithm in the determination of the noise parameters is not satisfactory for all noises except the QN and ARW for the data lengths used in the simulations. Therefore we can conclude that the choice of Fibonacci numbers for differencing intervals is not suitable especially for low frequency noise characterization.

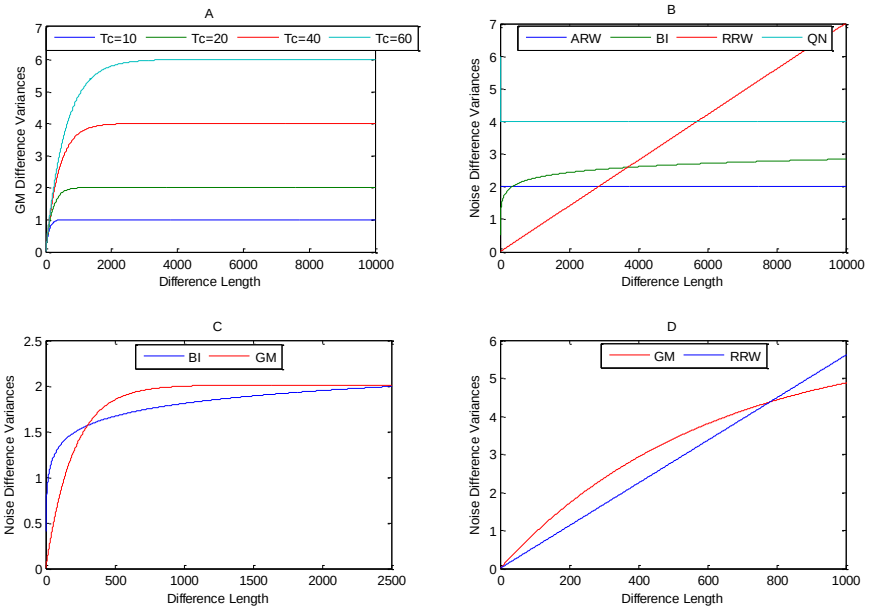

Figure 22: Difference variances for the noise sources at 10Hz. (A) Gauss Markov noise for different correlation times, (B) All other noise sources. Input noise variances GM=1, ARW=1, BI=4, RRW=0.07, QN=0.1 (C) BI 'variance=3.2' and GM 'variance=1, Tc=20' (D) RRW 'variance=0.5' and GM 'variance=1, Tc=60'

Correlation time of the GM noise changes the model matrix A radically. Estimation of the correlation time accurately will improve the performance of the estimation of the other parameters. The objective function is unfortunately neither a convex function of the correlation time nor its unimodal. So we have used quantized values of the correlation time and optimized other parameters for each level of the correlation time. The algorithm finds correlation time and other model parameters accurately for large data lengths.

During the simulations, up to now, Fibonacci numbers are used for difference values. Fibonacci sequence is selected only for its property of exponential increase which causes good estimation for high frequency noise components. This increase is necessary not to obtain a degenerate set of equations. The results are quite good even for real data as given in Figure 33, however for short data lengths the stationarity of the data is questionable and this causes convergence of the algorithm to some wrong values. To overcome this problem, difference values proposed in Section 5.1 can be used. It is shown in the following simulations that, the algorithm is more robust even for limited data when difference interval lengths are changed as proposed. The main disadvantage of the other methods is the increase of the calculation time compared to the Fibonacci numbers selection.

6.1 Step Wise Changing Interval Lengths

Previous experiment shows that the performance of the estimator can be improved by selecting interval lengths using a different strategy. At this section we have used the stepwise increase in the interval lengths. We have done 3 simulations in this part. For each simulation a different input noise difference is used.

Simulation 1.
Input noise parameters given in Table VI are used for this simulation. Correlation time for Gauss-Markov noise starts from 60 sec and reduces to 5 sec. For each correlation time inertial sensor outputs are generated using the simulator and input noise variances and correlation times are estimated using the proposed algorithm. Results are obtained and plotted in Figure 24. Convergence rate of ARW, QN and GM noise variances are estimated very well in a short time. Estimation of RRW and BI noise variances needs more time but converges to the expected value successfully. Correlation time of GM noise is estimated better when it is less than 20 sec.

Table VI: Parameters of Simulation1

Parameters	A^2	B^2	R^2	Q^2	G^2
Input Noise Variances	5	0.5	0.001	0.3	0.2

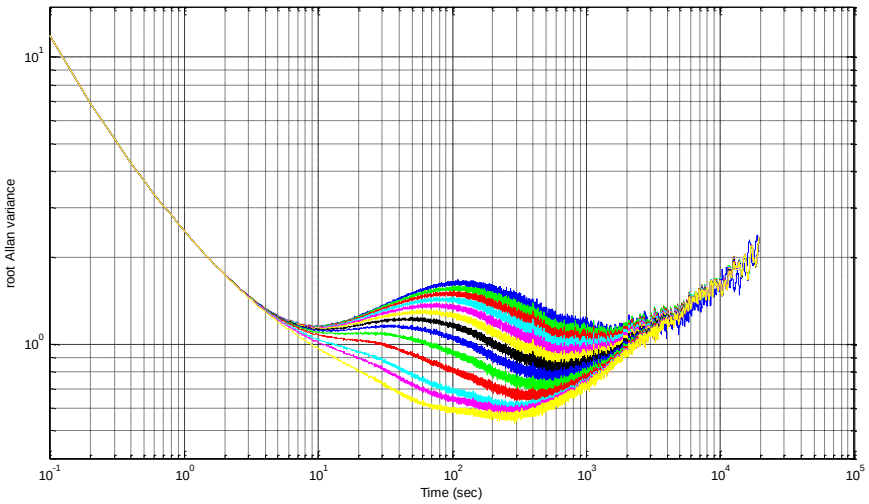

Figure 23: Allan variance plot for simulation 1

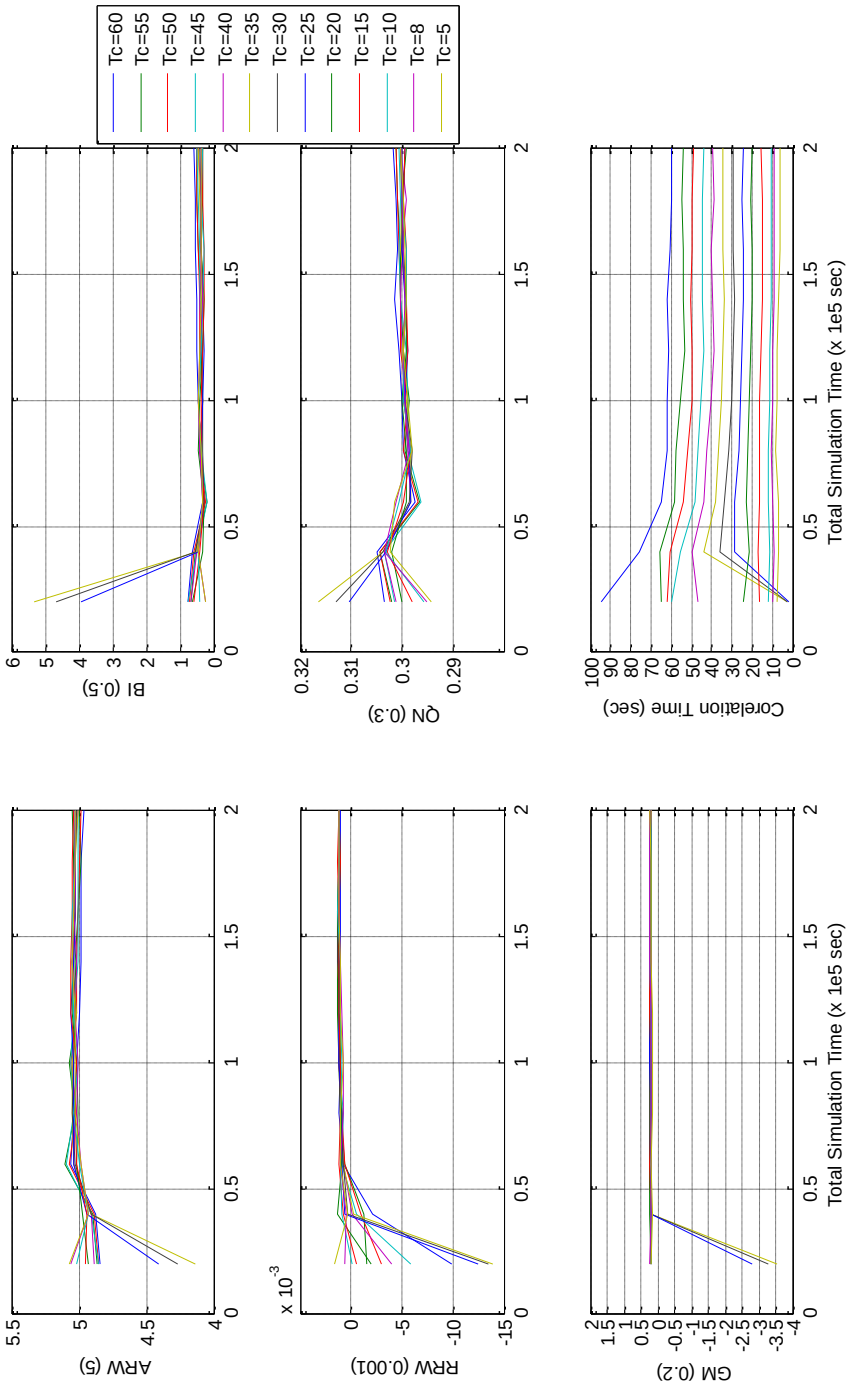

Figure 24: Stochastic error parameter estimations for correlation times, 5, 8, 10, 15, 20, 25, 30, 35, 40, 45, 50, 55, 60 sec and for different simulation times (Actual values are ARW=5, BI=0.5, RRW=0.001, QN=0.3, GM=0.2)

Allan variances for different correlation times are calculated and given in Figure 23. The figure shows that the artificial data generated is reasonable. The correlation time changes of the GM are clearly observed from the plot but however the computation of the BI parameter is almost impossible from it.

Simulation 2.
For this simulation input noise parameters are given in Table VII. Results are obtained and plotted in Figure 26. Related root Allan variance plot is given in Figure 25. Estimation performance and convergence rate of noise variances and correlation time are very similar to the previous simulation, except for BI noise variance. The reason for this is the very small value assigned for this noise variance.

Table VII: Parameters for Simulation 2

Parameters	A^2	B^2	R^2	Q^2	G^2
Input Noise Variances	1	0.07	0.0007	0.1	0.06

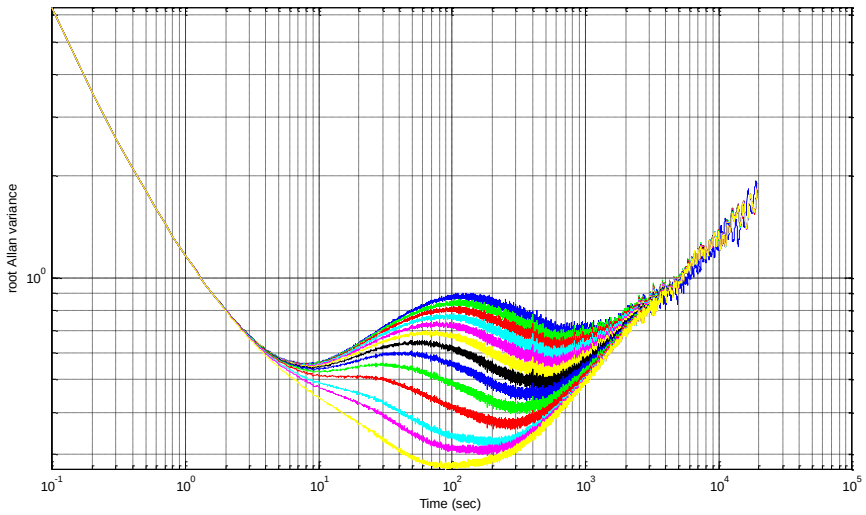

Figure 25: Allan variance plot for simulation 2

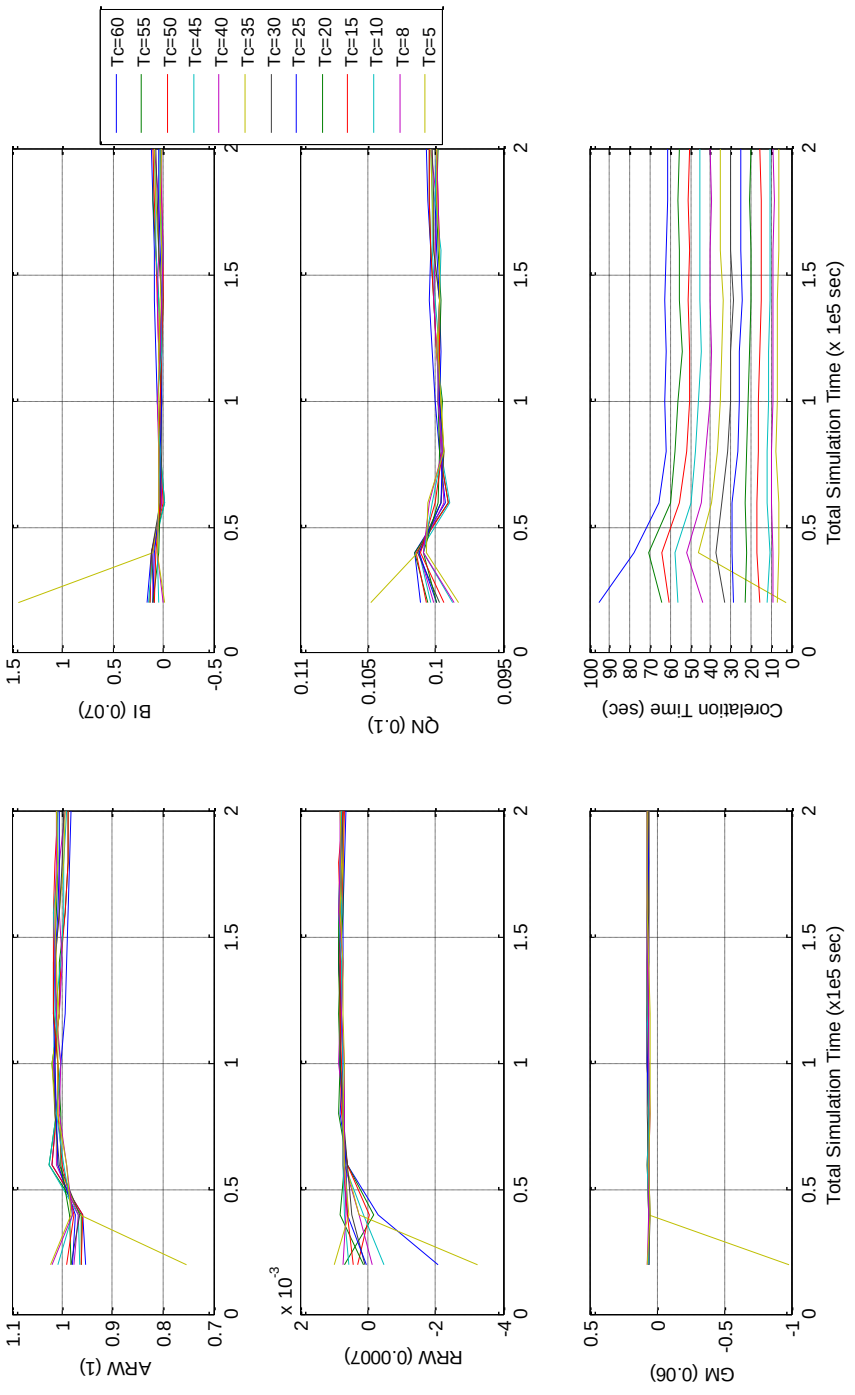

Figure 26: Stochastic error parameter estimations for correlation times, 5, 8, 10, 15, 20, 25, 30, 35, 40, 45, 50, 55, 60 sec and for different simulation times (Actual values are ARW=1, BI=0.07, RRW=0.0007, QN=0.1, GM=0.06)

Simulation 3.
For this simulation input noise parameters are given in Table VIII. Results are obtained and plotted in Figure 28. The corresponding root Allan variance plot is given in Figure 27. Estimation performance and convergence rate of noise variances and correlation time are very similar to the previous simulations. In this simulation GM and RRW noise variances are small. Results are very satisfactory in terms of estimation performance and convergence rate.

Table VIII: Parameters for Simulation 3

Parameters	A^2	B^2	R^2	Q^2	G^2
Input Noise Variances	1	0.5	0.0003	0.2	0.1

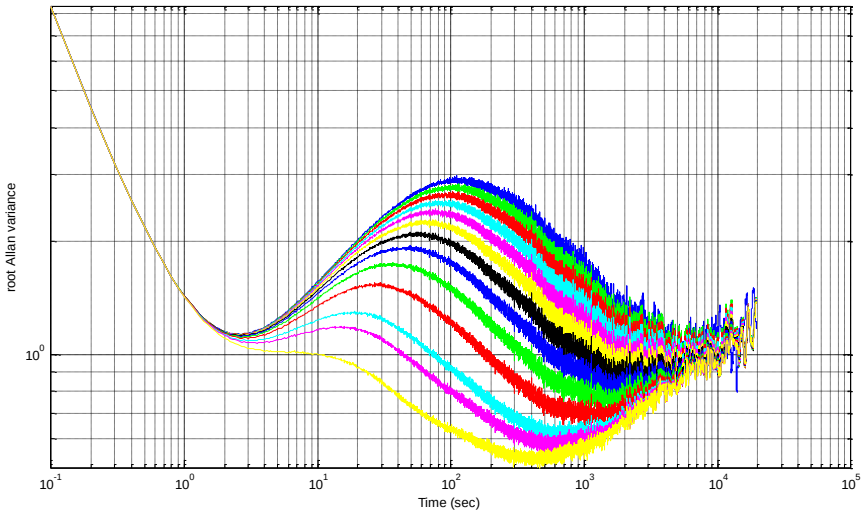

Figure 27: Allan variance plot for simulation 3

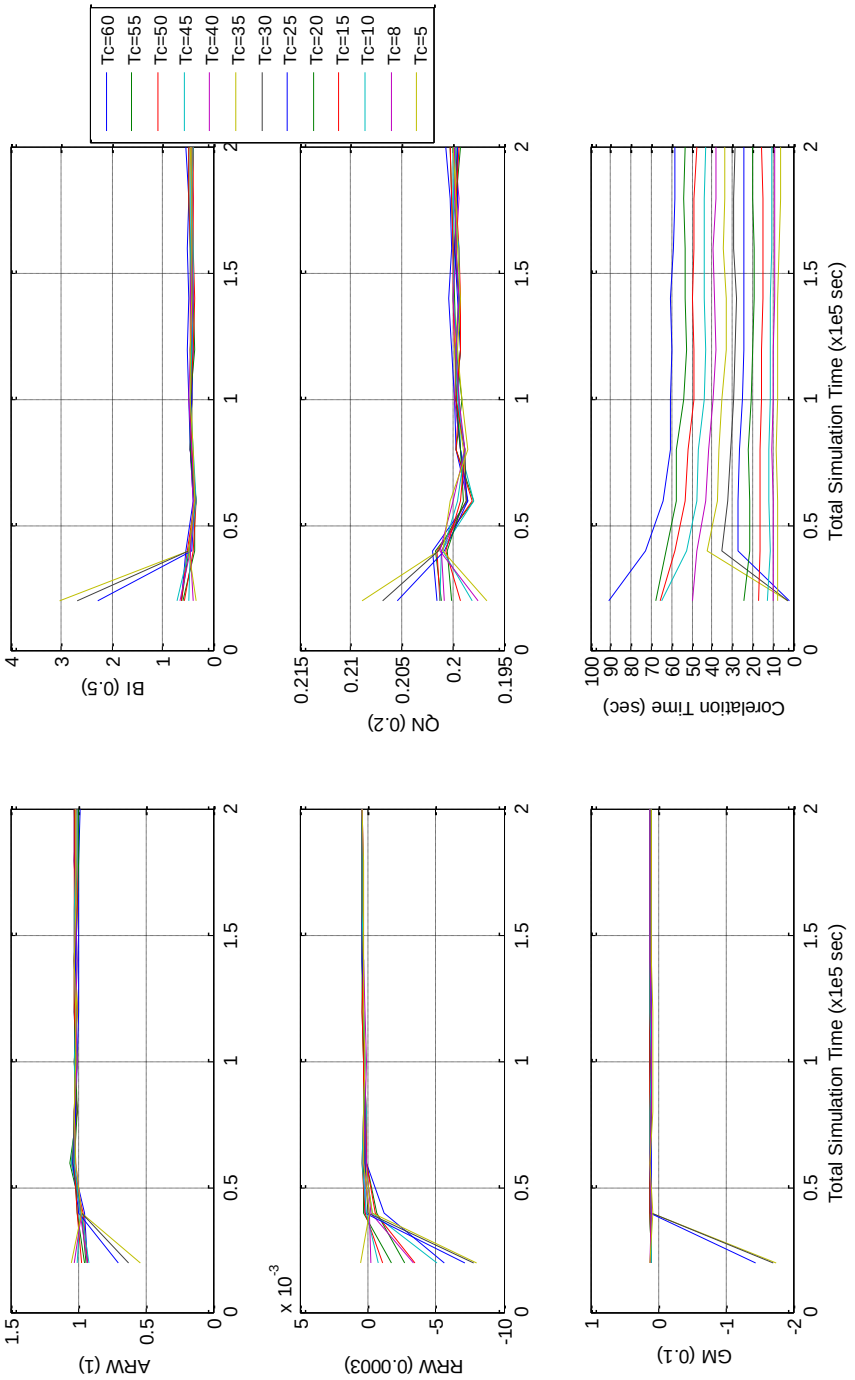

Figure 28: Stochastic error parameter estimations for correlation times, 5, 8, 10, 15, 20, 25, 30, 35, 40, 45, 50, 55, 60 sec and for different simulation times (Actual values are ARW=1, BI=0.5, RRW=0.0003, QN=0.2, GM=0.1)

Generally, high frequency noise parameters namely the angle random walk and the quantization noise parameters are accurately estimated, independent of the simulation time and the GM correlation time. Estimation of the bias instability and the rate random walk are badly affected from short data lengths. GM noise variance estimate is closely related with the accuracy of its correlation time estimate. For high GM correlation time, accuracy of it reduces and all of the low frequency noise source parameter estimation accuracies are affected accordingly.

We can say that the proposed new method finds the stochastic model parameters namely QN, ARW, BI, RRW, GM noise and GM correlation time successfully. It also finds small noise variances that cannot be determined from the Allan variance plot. Increasing the number of difference variances increases the convergence rate of the algorithm. In other words, parameters determined with less data.

Using limited number of difference variances improves the calculation time considerably. The calculation time of the new method is at least 80 times less than the computation time of the Allan variance.

For high GM correlation times, convergence performance of the algorithm is reduced. The main reason for this is the high sensitivity of the related column (i.e. GM noise covariance) of the input matrix to the correlation time.

The online estimation technique, explained in [2], can also be compared with our approach. The main advantage of our method over the online estimation technique is the richer set of estimated noise variances. Reduction in the calculation complexity is the second advantage of the proposed method over the online estimation technique given in [2].

Finally when the estimated parameters are too small or inefficient number of samples is used, estimated variances may become negative. In this case related column can be deleted and the similar least squares estimation method may be applied for the other unknown noise variances.

6.2 Interval Lengths Changing with Square Function

Simulation 1.
For this simulation input noise parameters given in Table IX are used. Correlation time for Gauss-Markov noise range is 10-60 sec. Estimated input noise parameters for different data lengths and for different correlation times are given in Figure 29. Difference sequence used for these simulations is obtained using the quadratic function as explained in Section 5.1.

Table IX: Input Noise Parameters

Parameters	A^2	B^2	R^2	Q^2	G^2
Input Noise Variances	1.9	0.7	0.005	0.5	0.6 Tc is variable

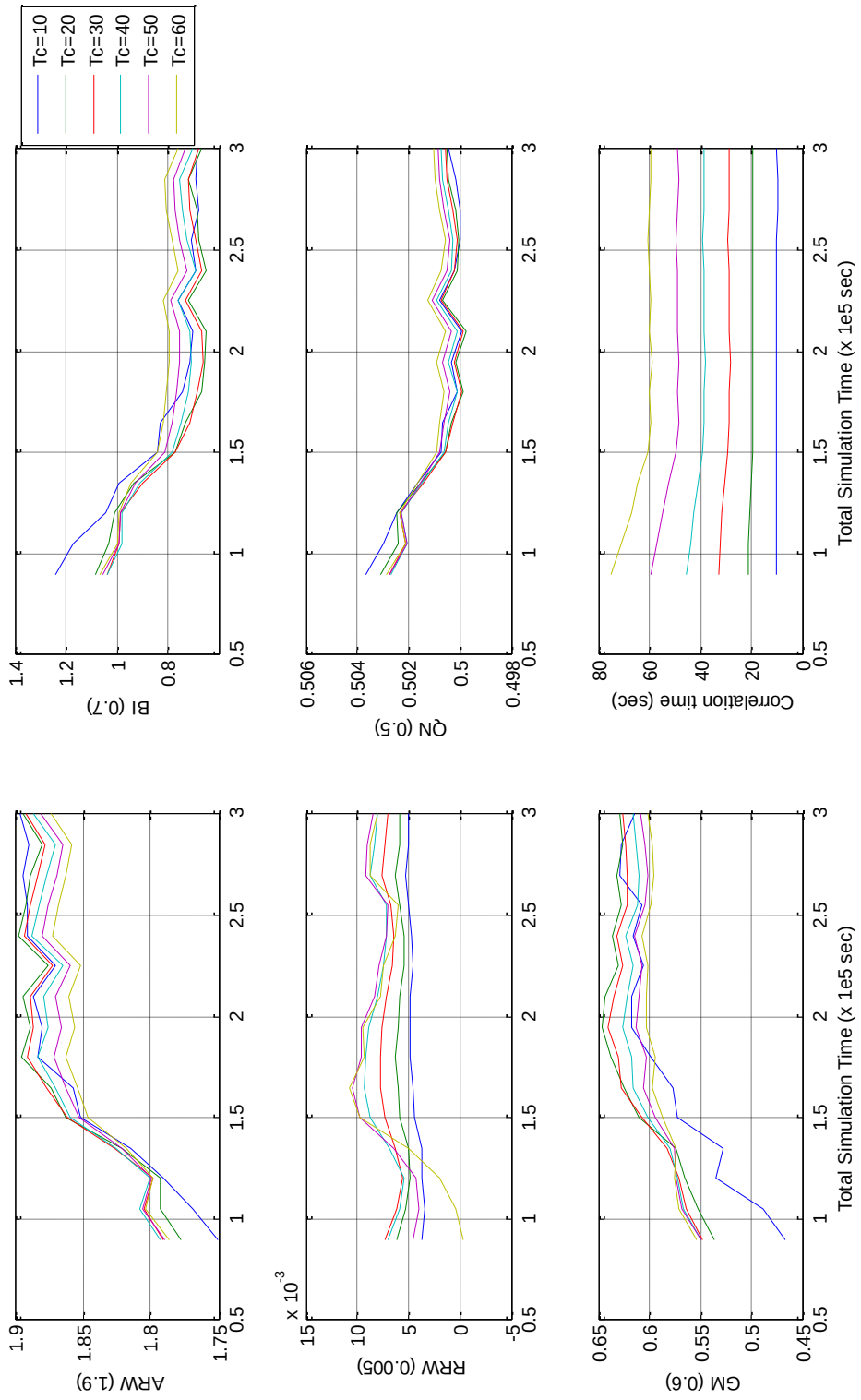

Figure 29: Stochastic error parameter estimations for different correlation times, 10, 20, 30, 40, 50, 60 sec and for different simulation times (Actual values are ARW=1.9, BI=0.7, RRW=0.005, QN=0.5, GM=0.6)

One interesting result is that all of the estimations are worse for small data lengths when the correlation times are small. Quadratic function of the delays does not provide good resolution for high frequency noise terms, QN, ARW and low correlation time GM noises. The main reason for this is the insufficient number of small delay values. Performance of the estimation increases while the simulation time increases. Similarly, other noise parameter estimation accuracies are better for long simulation times in general.

Simulation 2 and Simulation 3.

The input noise parameters given in Table X are used for the following two simulations. Correlation time range is 10-60 sec. for the Gauss-Markov noise.

Table X: Input Noise Parameters

Parameters	A^2	B^2	R^2	Q^2	G^2
Input Noise Variances Simulation 2	1	0.1	0.005	0.1	0.05 Tc is variable
Input Noise Variances Simulation 3	1	0.5	0.0003	0.2	0.1 Tc is variable

Simulation results given in Figure 30 and Figure 31 demonstrate the similarity between the new simulations and the previous one. One of the important conclusions is about the steady state performance. The degradation in the performance even for long data length is due to the variation of the difference variances for finite data length. Automatic averaging made by the stepwise function remove this effect considerably, providing better convergence performance as compared to the quadratic function.

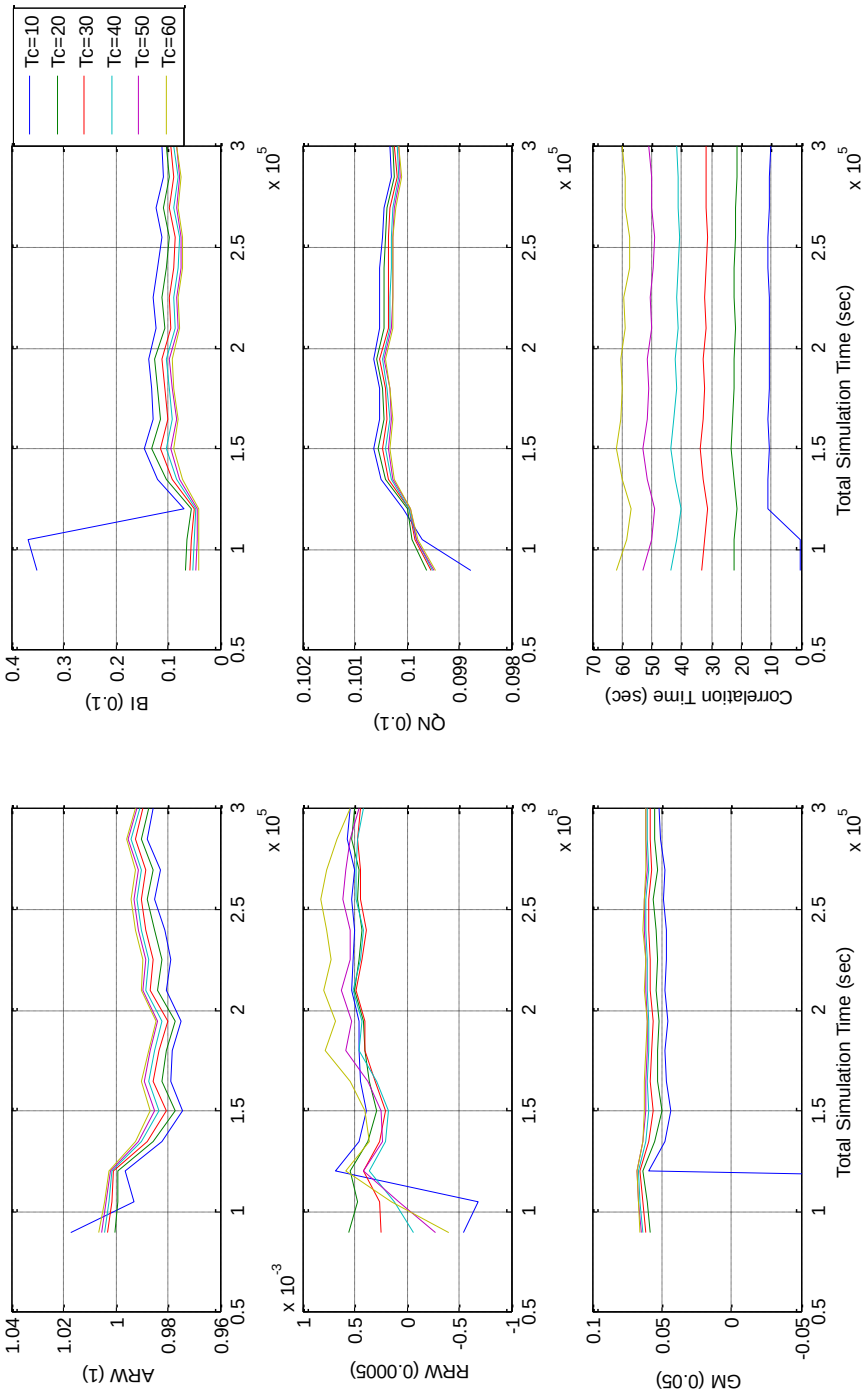

Figure 30: Error parameter estimations for different correlation times, 10, 20, 30, 40, 50, 60 sec and for different simulation times (Actual values are ARW=1, BI=0.1, RRW=0.005, QN=0.1, GM=0.05)

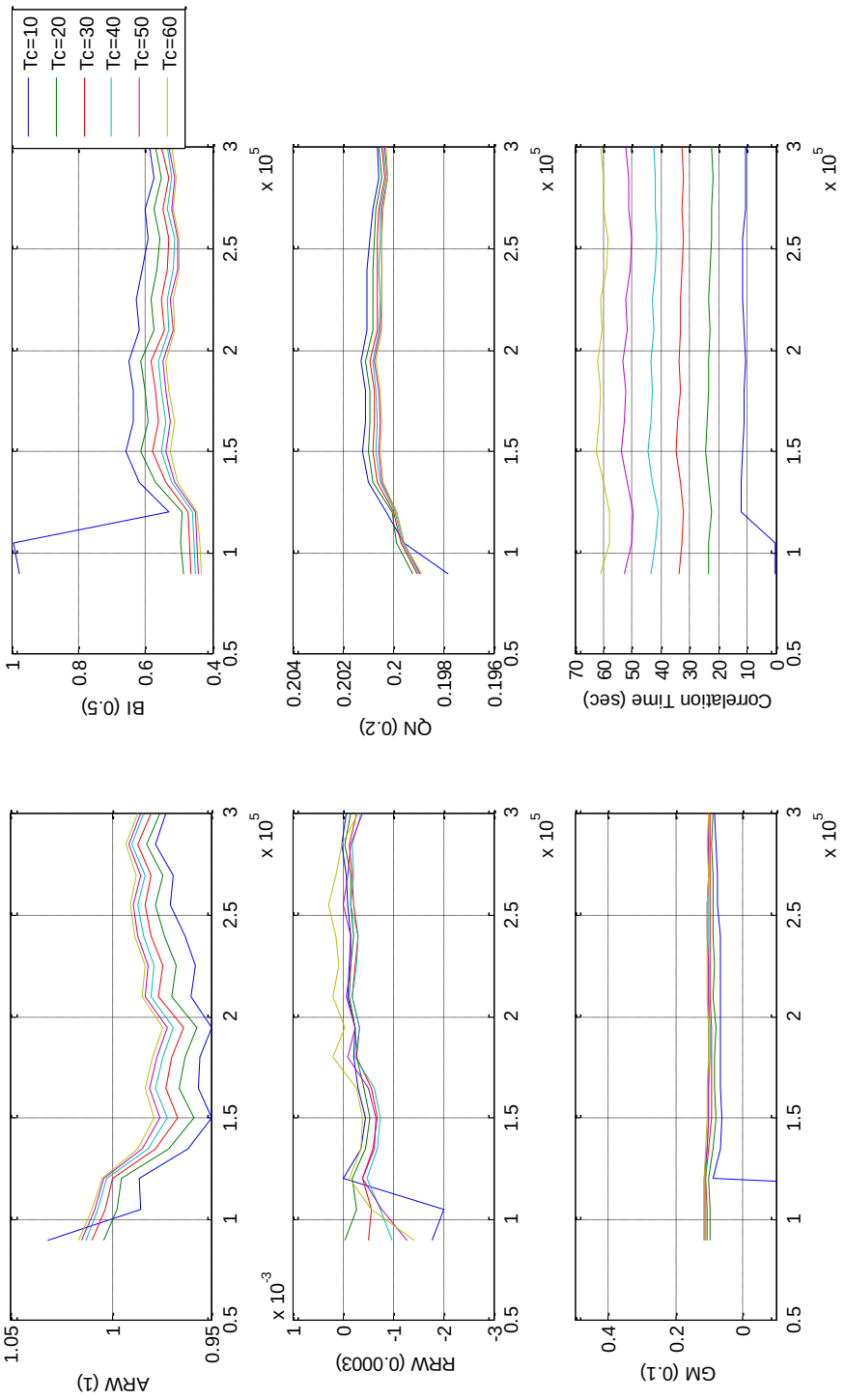

Figure 31: Error parameter estimations for different correlation times, 10, 20, 30, 40, 50, 60 sec and for different simulation times (Actual values are ARW=1, BI=0.5, RRW=0.0003, QN=0.2, GM=0.1)6.3 Application to the Real Data

The real data used in this study is obtained from 13 different sensors. Each IMU has three gyroscope and three accelerometer outputs and all the sensors are tactical grade. IMU1 sensor outputs are acquired for two hours with 10 Hz sampling rate and IMU2 sensor outputs are acquired for six hours with 1 Hz sampling rate. Except for the third accelerometer, subjected to the gravitational field, all sensor outputs can be considered as zero input for both IMU. Finally, a single accelerometer output which is acquired for 7 hours with 10 Hz sampling rate is subjected to the gravitational field. Summary of the real data used in this study is given in Table XI.

Table XI: Summary of the Real Data Used

Real Sensor Data		Data Rate (Hz)	Simulation Time	Input
IMU1	**Gyroscope1,2,3**	10	2 hours	0
	Accelerometer1,2	10	2 hours	0
	Accelerometer3	10	2 hours	1g
IMU2	**Gyroscope1,2,3**	1	6 hours	0
	Accelerometer1,2	1	6 hours	0
	Accelerometer3	1	6 hours	1g
Accelerometer		10	7 hours	1g

In order to verify the method on the real inertial sensor data, the output of the MEMS accelerometer data sampled at 10Hz and acquired approximately 7 hours. The output of the sensor in mg is given in Figure 32. Stochastic model parameters are determined using the proposed algorithm and are listed in Table XII. Note that during these calculations delay times are selected as 'stepwise difference'.

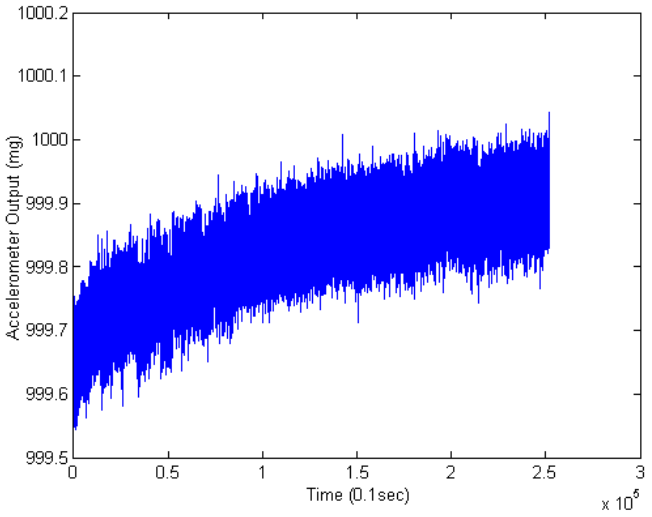

Figure 32: Output of the real MEMs sensor

Table XII: Calculated Stochastic Model Parameters of the MEMs sensor by using the proposed algorithm

Parameters	A^2	B^2	R^2	Q^2	G^2
Values computed by the proposed method	911.54e-6	103.94e-6	1.85e-6	0	64.95e-6 (Tc=31.05)

To test the correctness of the estimated values the two Allan variance plots; the Allan variance plot of the original data and the data generated by using the estimated stochastic model parameters are compared with each other. The result is given in Figure 33. The similarity of the two plots shows that the noise parameters are estimated quite well.

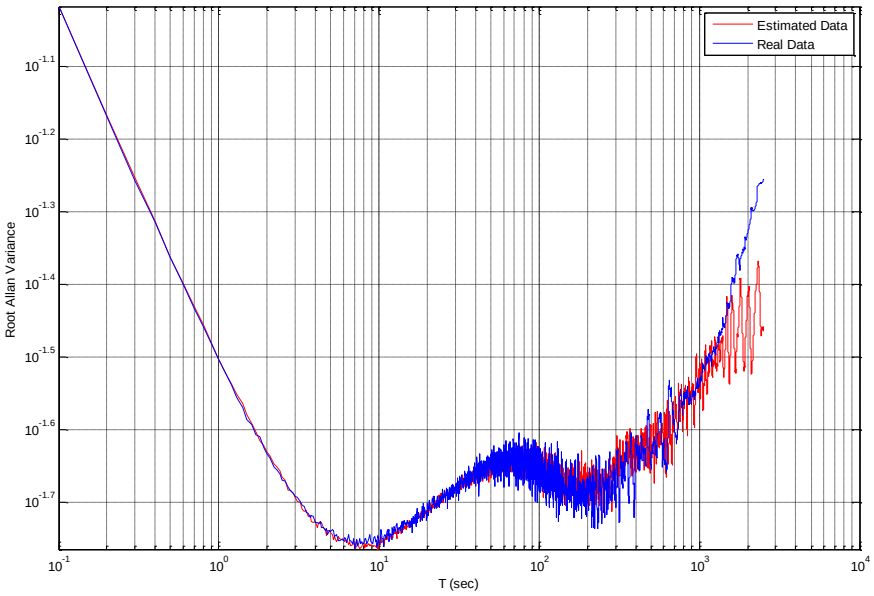

Figure 33: Allan Variance of real sensor output (blue) and estimated sensor output (red)

CHAPTER 7

INDIVIDUAL NOISE CHARACTERIZATION

The devices and systems that have $1/f^{\alpha}$ type noises have been observed over the years. This type of noise arises in resistance and thermal fluctuations, voltages across vacuum tubes and diodes, and almost every solid state device, frequency fluctuations in oscillator, and voltages in most superconducting devices. There are lots of fields other than physics and engineering; like economics, music, weather, traffic and hydrology that this noise source can be observed, [6]. Therefore modeling and identification of this type of noise sources have crucial importance in many fields.

The devices and systems that have $1/f^{\alpha}$ type noises have been observed over the years. This type of noise arises in resistance and thermal fluctuations, voltages across vacuum tubes and diodes, and almost every solid state device, frequency fluctuations in oscillator, and voltages in most superconducting devices. There are lots of fields other than physics and engineering; like economics, music, weather, traffic and hydrology that this noise source can be observed as given in [6]. Therefore modeling and identification of this type of noise sources have crucial importance in many fields.

In this chapter of the thesis, the effectiveness of the proposed method in determination of the individual noise source parameters will be shown. In order to do this, the stochastic noise source models specified in Chapter 2 are used. In this model, five noise sources, QN, ARW, BI, RRW and GM, are given with their transfer functions. Except for the GM noise source, all the other models can be described by the output of the white noise source with the transfer function H(z), written by;

$$H(z) = \frac{sr^{\frac{\alpha}{2}}}{\left(1 - z^{-1}\right)^{\frac{\alpha}{2}}} \tag{54}$$

In order to get the QN from this transfer function α is set to -2. Similarly, α is set to 0 for ARW, 1 for BI and 2 for RRW. Besides these noise sources different noise sources can be generated and identified using this model with all rational values of α between -2 and +2. Therefore, different types of noise models can be generated and characterized using the proposed new method.

Gauss Markov noise, on the other hand, is different from the $1/f$ type noise sources, in that, coefficient of z^{-1} term is not unity and equal to $e^{-\frac{sr}{Tc}}$. The parameter α is equal to 2 for the first order GM noise. Therefore its generation and identification is explained in different subtitles.

7.1 Generation of 1/f$^{\alpha}$ Noise Source

Generation of $1/f^{\alpha}$ noise is explained for α is equal to one, previously. The autoregressive transfer function is chosen for this purpose. Input white noise is filtered using the transfer function, $H(z)$, where it is equal to;

$$H(z) = \frac{sr^{\frac{\alpha}{2}}}{\left(1 - z^{-1}\right)^{\frac{\alpha}{2}}} = \frac{sr^{\frac{\alpha}{2}}}{h_0 + h_1 z^{-1} + h_2 z^{-2} + \ldots} \tag{55}$$

where,

$$\begin{aligned} h_0 &= 1 \\ h_k &= \left(k - 1 - \frac{\alpha}{2}\right)\frac{h_{k-1}}{k} \end{aligned} \tag{56}$$

as given in [6].

Allan variance can be used to show the effect of this filtering. For α is equal to zero $H(z)$ becomes unity. The values chosen for α are 0.3, 0.5, 0.8, 1, 1.5, 2. White noise has unit variance and sampling rate is set to 0.1 sec for the simulations. The order of filter is increased up to 20000.

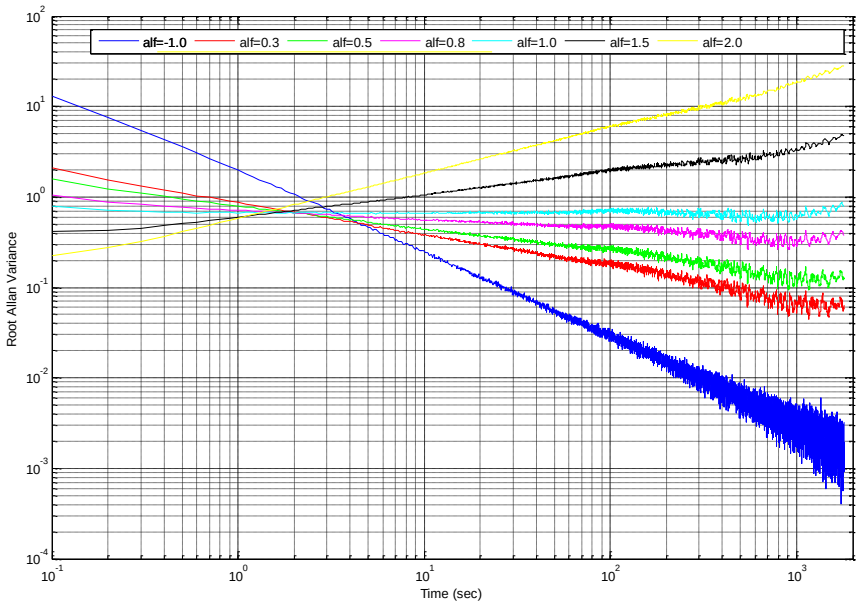

Figure 34: Root Allan Variance of 1/f$^{\alpha}$ noise

The generated noise characteristics are as expected and given in the root Allan variance plot in Figure 34.

Note that in the generation of this type of noise sources, AR model of $H(z)$ is preferred. Because of the nature of the proposed algorithm for determination of the unknown noise parameters, which depends mainly on the variance of differences, the moving average model of $H(z)$ is preferred.

7.2 Characterization of 1/f$^{\alpha}$ Noise Source

Stochastic noise sources of the form $1/f^{\alpha}$ can be characterized with two parameters, α and the input white noise variance. Our aim here is to identify these two parameters from the generated noise sources explained in the previous section. The effect of sampling rate is also took account.

The transfer function used to characterize the noise source can be expanded as moving average form and given in Eq.57.

$$H(z)=\frac{sr^{\frac{\alpha}{2}}}{\left(1-z^{-1}\right)^{\frac{\alpha}{2}}}=sr^{\frac{\alpha}{2}}\left(h_0+h_1z^{-1}+h_2z^{-2}+...\right) \tag{57}$$

where,

$$\begin{aligned} h_0 &= 1 \\ h_k &= \left(k-1+\frac{\alpha}{2}\right)\frac{h_{k-1}}{k} \end{aligned} \tag{58}$$

In this model, output of the system x_k can be obtained by filtering the white noise ω_k with $H(z)$, given in [6].

$$x_k=\left(h_0\omega_k+h_1\omega_{k-1}+h_2\omega_{k-2}+...\right)sr^{\frac{\alpha}{2}} \tag{59}$$

If the input noise variance for ω_k is σ^2 then the difference variances can be obtained as.

$$\mathrm{var}(x_k-x_{k-n})=\left(h_0^2+h_1^2+...+h_{n-1}^2+\left(h_n-h_0\right)^2+\left(h_{n+1}-h_1\right)^2+...\right)\sigma^2sr^{\alpha} \tag{60}$$

Difference variances is a function of σ, sr and α. In order to remove the effect of σ and sr, variances can be normalized with respect to the first difference variance. In other words;

$$\frac{\mathrm{var}(x_k-x_{k-n})}{\mathrm{var}(x_k-x_{k-1})}=\frac{\left(h_0^2+h_1^2+...+h_{n-1}^2+\left(h_n-h_0\right)^2+\left(h_{n+1}-h_1\right)^2+...\right)}{\left(h_0^2+\left(h_1-h_0\right)^2+\left(h_2-h_1\right)^2+...\right)} \tag{61}$$

Note that h_i values is a function of α for i>0. Therefore using the equation specified in (25), one can easily determine the critical parameter α for characterization of the noise source using a gradient base optimization algorithm. However, if the cost function plots

given in Figure 35 and Figure 36 are examined, golden section selection algorithm converges to the solution accurately and effectively. Determination of the input noise variance is very simple if α is known. Note that, sampling rate is always a known parameter for this identification problem.

The cost function that is minimized for the parameter α can be formulized as in Eq.61 and 30 diffrence variances (i.e. k=30) are used during the simulations.

$$\min_{\alpha} \sum_{n=1}^{k} \left(\left(\frac{\left(h_0^2 + h_1^2 + ... + h_{n-1}^2 + \left(h_n - h_0\right)^2 + \left(h_{n+1} - h_1\right)^2 + ...\right)}{\left(h_0^2 + \left(h_1 - h_0\right)^2 + \left(h_2 - h_1\right)^2 + ...\right)} \right) - \left(\frac{\mathrm{var}\left(gf\left(n\right)\right)}{\mathrm{var}\left(gf\left(1\right)\right)} \right) \right)^2 \quad (62)$$

where, *gf*(*n*) is calculated by taking the variance of the sequence obtained from the difference of the original sequence and its *n* delayed version. Determination of the parameter α is quite simple using golden section selection algorithm.

Once α is determined a simple least square estimation technique can be applied to identify the input noise variance, as given in Eq.63 and Eq.64,

$$\min_{\sigma} \sum_{n=1}^{k} \left(\left(h_0^2 + h_1^2 + ... + h_{n-1}^2 + \left(h_n - h_0\right)^2 + \left(h_{n+1} - h_1\right)^2 + ...\right) \sigma^2 sr^{\alpha} - \mathrm{var}\left(gf\left(n\right)\right) \right)^2 \quad (63)$$

and,

$$\sigma_{LSE}^2 = \frac{1}{sr^{\alpha}} \begin{bmatrix} \left(h_0^2 + \left(h_1 - h_0\right)^2 + \left(h_2 - h_1\right)^2 + ...\right) \\ \left(h_0^2 + h_1^2 + \left(h_2 - h_0\right)^2 + \left(h_3 - h_1\right)^2 + ...\right) \\ ... \\ \left(h_0^2 + h_1^2 + ... + h_{n-1}^2 + \left(h_n - h_0\right)^2 + \left(h_{n+1} - h_1\right)^2 + ...\right) \end{bmatrix}^T \begin{bmatrix} gf\left(1\right) \\ gf\left(2\right) \\ ... \\ gf\left(n\right) \end{bmatrix} \quad (64)$$

In other words, dependence of the input noise variance is excluded from the algorithm by normalization and the parameter α is identified first. Then input noise variance is determined using a simple least square estimation method.

In the following subsection the algorithm details are given and its performance is shown by the simulations.

7.3 Simulations for Identification of 1/f$^{\alpha}$ Noise

The technique for generation and characterization of the 1/fα noise source is explained in detail previously. According to this, different noise sources are generated and its suitability will be discussed. Next, the two unknown parameters, α and σ^2, to characterize the noise source is identified using the proposed algorithm for each noise source.

Before going further, it is better to examine the cost function specified in (26) for different values of α between -2 to +2. For α is greater than 1 than the gradient of the cost function increases as shown in Figure 35. If the same figure is plotted to see the effect of the α which is less than one, cost function axis is limited between zero and one and plotted in Figure 36.

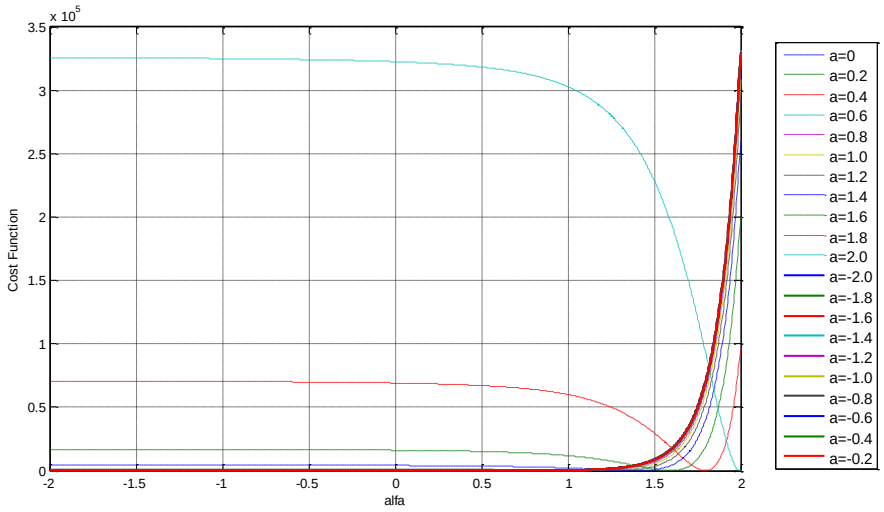

Figure 35: Cost Function Change While α Changes From -2 to 2

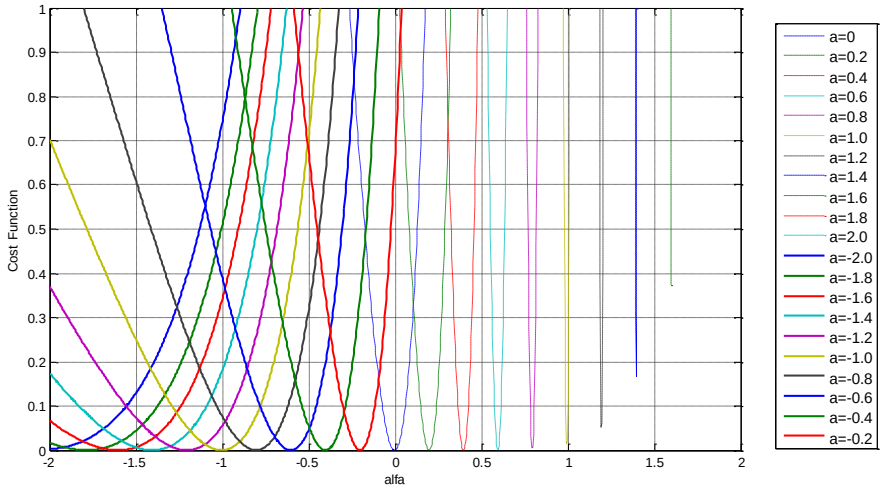

Figure 36: Cost Function Change While α Changes From -2 to 2 with Axis Limitation

These two figure shows that cost is a convex function of α, gradient of the cost function is small if α is less than one. This is the main reason why golden section selection algorithm is preferred instead of the gradient base approach.

For the first simulation, input parameters are chosen as α and σ^2 is equal to 1.5 and 0.5, respectively and a gradient base approach performance is shown. Gradient of the cost function is obtained by numerical differentiation. Convergence of the parameter α is given in Figure 37 and the results are obtained as in Table XIII. All of the simulations use

0.1 sec sampling time for both generation and therefore characterization of the noise. Total experiment time is 5 hours for the simulation.

Table XIII: Actual and Estimated Noise Parameters for 5 Hours Simulation Time

$1/f^{\alpha}$ noise	Actual	Estimated	İnitial Value
α	1.5	1.501	1
σ^2	0.5	0.499	-

From the graph convergence rate of the parameter α is quite good and 70 iterations are enough for the parameter to converge.

If total simulation time is reduced to an hour, then the accuracy of the result reduces but is acceptable as specified in Table XIV and the convergence rate remains unchanged as given in Figure 38.

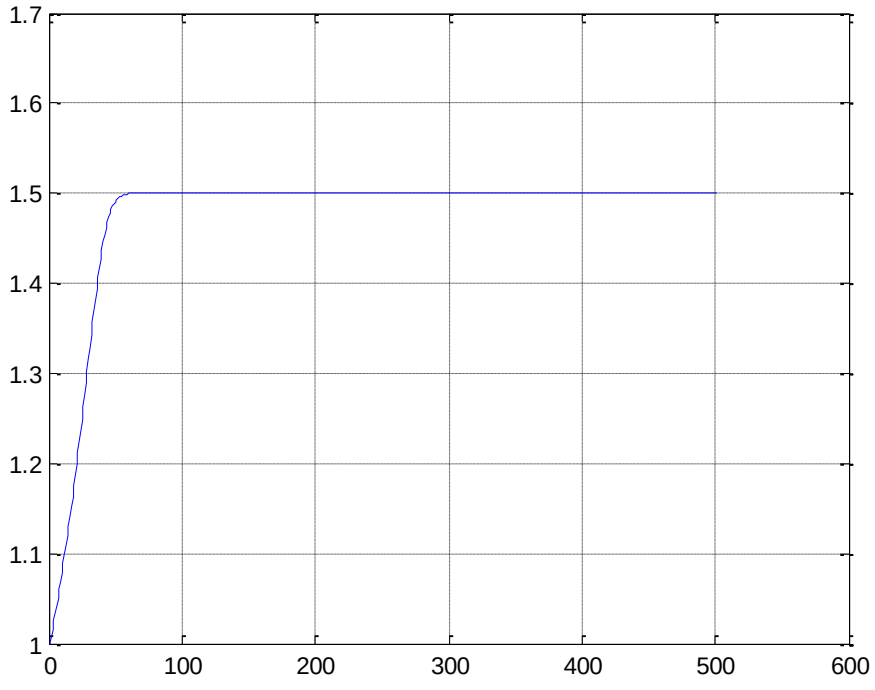

Figure 37: Convergence of the parameter α for 5 hours simulation time

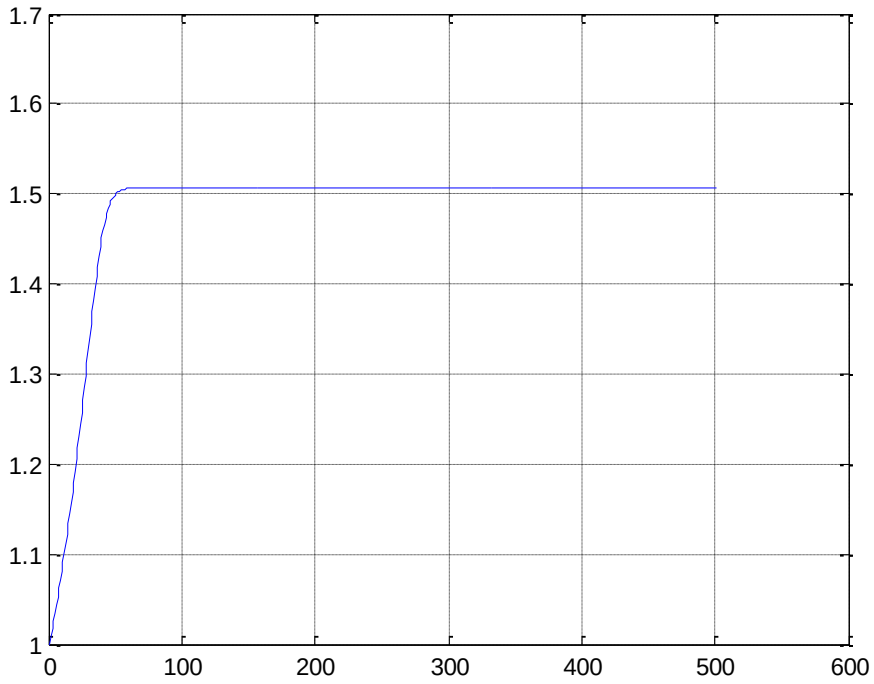

Figure 38: Convergence of the parameter α for 1 hour simulation time

Table XIV: Actual and Estimated Noise Parameters for 1 Hour Simulation Time

$1/f^{\alpha}$ noise	Actual	Estimated	İnitial Values
α	1.5	1.507	1
σ^2	0.5	0.500	-

For the remaining simulations 5 hours simulation time will be used and algorithm performance will be shown for different input parameters. The algorithm preferred to determine the parameter α is the golden section selection for these simulations. The main advantage for this algorithm is the performance related with the number of iteration and maximum error can easily be obtained from (65).

$$error \leq \frac{4}{1.618^N} \tag{65}$$

Where, N is the number of iteration. Note that the error is also related with the simulation time and therefore calculation of the difference variances. Sampling rate 0.1 sec is used for generation and estimation algorithms. The results are obtained for 100 iterations and listed in Table XV.

Table XV: Input and estimated noise parameters for 1/f$^{\alpha}$ noise

1/f$^{\alpha}$ noise	Actual	Estimated	1/f$^{\alpha}$ noise	Actual	Estimated
α	-1	-0.996	σ^2	0.5	0.507
α	-0.3	-0.303	σ^2	0.5	0.496
α	1.8	1.803	σ^2	0.3	0.301
α	1.5	1.500	σ^2	0.5	0.499
α	1.2	1.197	σ^2	0.1	0.010
α	0.5	0.498	σ^2	0.5	0.496
α	0.1	0.102	σ^2	0.5	0.505

7.4 Generation and Characterization of First Order Gauss-Markov Model

Generation of the Gauss-Markov (GM) noise is quite simple and obtained by filtering the white noise with the transfer function given in (66);

$$H(z) = \frac{sr}{\left(1 - e^{-\frac{sr}{Tc}} z^{-1}\right)} \tag{66}$$

where, sr is sampling rate and Tc is the correlation time of the GM noise. Input noise variance and the correlation time are the two parameters to characterize the first order GM noise. After the similar normalization process defined for 1/fα characterization dependence on input noise variance is removed from the problem and correlation time can be determined easily by a gradient base or golden section selection optimization algorithms. After normalization, the difference variances become as given in (67).

$$\frac{\mathrm{var}(x_k - x_{k-n})}{\mathrm{var}(x_k - x_{k-1})} = \frac{\left(1 - e^{-n\frac{sr}{Tc}}\right)}{\left(1 - e^{-\frac{sr}{Tc}}\right)} \tag{67}$$

Note that difference variances for GM noise can be obtained as in (68).

$$\mathrm{var}(x_k - x_{k-n}) = \frac{2\sigma^2 sr^2 \left(1 - e^{-n\frac{sr}{Tc}}\right)}{\left(1 - e^{-2\frac{sr}{Tc}}\right)} \tag{68}$$

Therefore the cost function that is minimized for the parameter Tc can be formulized as in (69). There are 3000 difference variances (i.e. k=3000) used for all simulations.

$$\min_{Tc} \sum_{n=1}^{k} \left(\frac{\left(1 - e^{-n\frac{sr}{Tc}}\right)}{\left(1 - e^{-\frac{sr}{Tc}}\right)} - \left(\frac{\mathrm{var}(gf(n))}{\mathrm{var}(gf(1))} \right) \right)^2 \tag{69}$$

Once Tc is determined a simple least square estimation technique can be applied to identify the input noise variance, as given in Eq. 69 and Eq. 70,

$$\min_{\sigma} \sum_{n=1}^{k} \left(\frac{2\sigma^2 sr^2 \left(1 - e^{-n\frac{sr}{Tc}}\right)}{\left(1 - e^{-2\frac{sr}{Tc}}\right)} - \mathrm{var}(gf(n)) \right)^2 \tag{70}$$

and,

$$\sigma^2_{LSE} = \frac{1}{2sr^2} \begin{bmatrix} \frac{2\sigma^2 sr^2 \left(1 - e^{-1\frac{sr}{Tc}}\right)}{\left(1 - e^{-2\frac{sr}{Tc}}\right)} \\ \frac{2\sigma^2 sr^2 \left(1 - e^{-2\frac{sr}{Tc}}\right)}{\left(1 - e^{-2\frac{sr}{Tc}}\right)} \\ \cdots \\ \frac{2\sigma^2 sr^2 \left(1 - e^{-n\frac{sr}{Tc}}\right)}{\left(1 - e^{-2\frac{sr}{Tc}}\right)} \end{bmatrix}^T \begin{bmatrix} gf(1) \\ gf(2) \\ \cdots \\ gf(n) \end{bmatrix} \tag{71}$$

7.5 Simulations for GM Noise

The algorithm proposed to identify the GM noise parameters using difference variances is slightly different from the $1/f^{\alpha}$ noise characterization, in that, GM noise characterization requires high difference values as compared to $1/f^{\alpha}$ noise. The parameter α is directly determined from the algorithm as shown previously. However for the GM noise instead of the correlation time, exponential function $e^{-\frac{sr}{Tc}}$ is determined first than the correlation time is evaluated. The reason for this is the reduced number of calculations. Golden section selection algorithm is also a good in determination of this parameter. Number of iteration

is chosen as 100 during the simulations. Sampling time of 0.1sec is used for generation of the GM noise.

Table XVI: Input and estimated noise parameters for GM noise

GM noise	Actual	Estimated	GM noise	Actual	Estimated
Tc	30	28.80	σ^2	0.5	0.500
Tc	60	60.53	σ^2	0.5	0.499
Tc	60	59.13	σ^2	0.1	0.998
Tc	20	19.47	σ^2	0.25	0.250
Tc	10	10.07	σ^2	0.25	0.250

Accuracy of the algorithm is quite good according to the simulations. Difference variances are calculated and taken account in the algorithm for all values from 1 to 3000. This increases the calculation time too much. The similar accuracy can also be obtained by selecting suitable difference values which results in a very short calculation time.

As a result we have concluded that the proposed difference variance method is a very good approach in determination of individual noise characterization. The only limitation related with this characterization is the prior information required for the noise whether it is GM or not.

CHAPTER 8

STOCHASTIC MODELLING USING ANGLE RANDOM WALK AND GAUSS MARKOV NOISE MODELS

In aided inertial navigation system design, Angle Random Walk (ARW) and Gauss-Markov (GM) noise sources are used in order to model gyroscope and accelerometer stochastic models frequently. The other noise sources, specified previously, are generally excluded from the model. The main reason for using only two noise sources for the whole stochastic model is the simplicity in the implementation of the Kalman filter error propagation equations. Similarity of the stochastic models of GM noise with the flicker noise and the rate random walk noise sources makes this approach meaningful.

Nonstationary noise sources are not suitable for error state propagation in Kalman filter. The variance of a nonstationary noise can not be predicted and therefore its use in the Kalman filter results in different propagation error at each run, independent of the application. This is the reason of using only the ARW and the GM noise models in most of the Kalman filter applications.

The non stationary noises BI and RRW are generated by two independent white noise sources in our model as suggested in the literature. We use the approximation of first order GM noise model for these noises. Input white noise variance, correlation time and the sampling rate are the three parameters required to model the GM noise in discrete time. Since the sampling rate is fixed, the other two parameters must be identified to characterize the BI or RRW noise sources.

Second order GM noise model can also be used to model the BI or RRW noise sources. But using only one second order GM model,to characterize the sensor output containing both BI and RRW noise sources will not be efficient due to the inherent independence of these two noises.

In this part of the study, the proposed new method will be used to approximate the inertial sensor stochastic model with ARW and GM noise models.

8.1 Simplified Stochastic Model and The Algorithm

Performance of the proposed new method was discussed for almost complete stochastic model for the inertial sensors, previously. In this complete model, there are five noise sources namely; QN, ARW, BI (flicker), GM and RRW. Generation of these noise sources forming the inertial sensor output is shown in Figure 39.

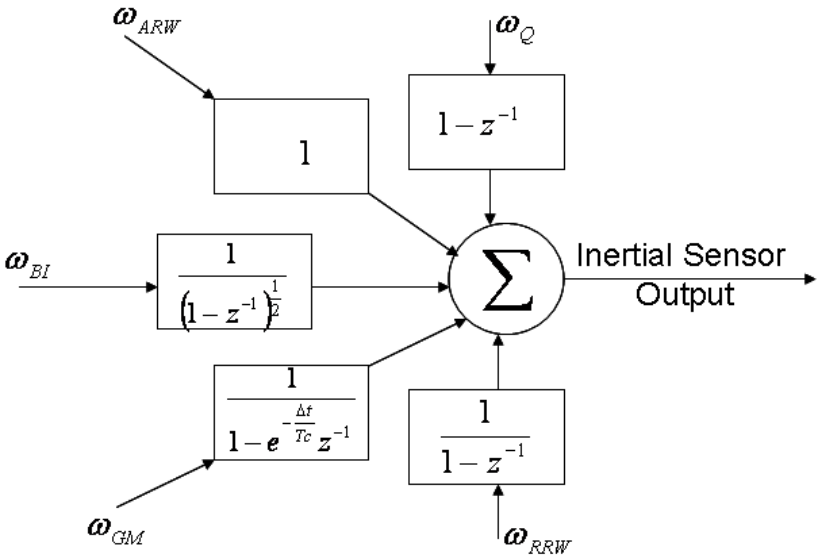

Figure 39:Stochastic Model Used in This Study

In this model mainly five noise covariances and the correlation time of the GM noise must be identified using the Least Square Estimation techniques. It is shown that, the performance in terms of accuracy and calculation time the proposed method is better than the Allan variance technique.

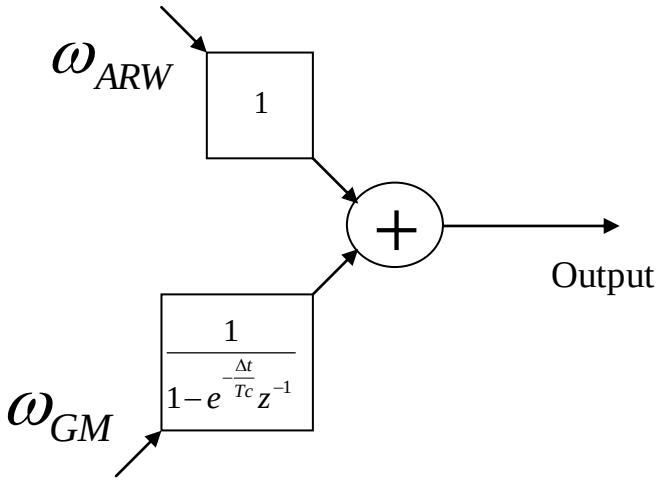

Figure 40: Simplified Model

A simplified model is shown in Figure 40. There are two noise sources that are represented by three parameters to be determined in this figure. The Gauss Markov model is used to model the flicker noise or the rate random walk noise or their combination. The reason for this is the similarity between the stochastic characteristics of

GM noise with the flicker noise and the rate random walk noise for different GM correlation time and for definite time interval.

Let g be the DC bias free output of the gyroscope that contains ARW and GM noise only. Then;

$$g_k = \omega_k^{ARW} + \omega_k^{GM} \tag{72}$$

where,

ω^{ARW} : Angle Random Walk noise (zero mean gaussian white) with σ^2_{ARW} variance

ω^{GM} : Gauss Markov noise obtained from the following process;

$$\omega_{\mathrm{k}}^{\mathrm{GM}} = e^{-\frac{sr}{T_C}} \omega_{k-1}^{GM} + \omega_k^{W}$$

where;

sr : .Sampling rate

T_c : Correlation time

ω^{W} : zero mean gaussian white noise with σ^2_{GM} variance

If variance of the difference sequence obtained from the g and its delayed versions is evaluated similar to the generalized model, the following matrix equation can be obtained. In order to simplify the equations

$$\begin{bmatrix} 2 & gm(1) \\ 2 & gm(2) \\ \dots & \dots \\ 2 & gm(n) \end{bmatrix} \begin{bmatrix} \sigma^2_{ARW} \\ \sigma^2_{GM} \end{bmatrix} = \begin{bmatrix} \mathrm{var}(g_{d1}) \\ \mathrm{var}(g_{d2}) \\ \dots \\ \mathrm{var}(g_{dn}) \end{bmatrix} \tag{73}$$

where;

$$gm(i) = 2 \frac{\left(1 - e^{-\frac{isr}{TC}}\right)}{\left(1 - e^{-\frac{2sr}{TC}}\right)} \tag{74}$$

and the sequence g_{di}, is obtained from the original sequence g and its i delayed versions by taking the difference. The three parameters to be determined do not form a convex or a unimodal objective function. However when the value of Tc is known the simple least squares gives the variance parameters of the ARW and the GM noises as before. The optimization method used in this work for Tc is a simple grid search.

The method is applied to the IMU1 and IMU2 data given in Table XI. There are three gyroscopes and three accelerometers data for each IMU. The performance of the algorithm is measured by comparing the Allan variance plots of the original data and the data generated from the estimated noise parameters. As stated before, some precautions

must be taken for the absence of some noise types. If the data has no GM noise component the algorithm may converge to negative variances or very large correlation times. In these cases GM noise variance is equated to zero and only ARW noise variance is estimated which is the case for the gyroscope outputs.

In order to estimate the parameters of the GM noise, difference values are increased up to one twentieth of the data length. If the data length is very large difference variances can be evaluated for the predefined delay times depending on the calculation time and the accuracy requirement.

8.2 Simulations

The first simulation shows the accuracy of the algorithm for the simplified model. ARW and the RRW noise sources are generated in order to simulate the sensor output. Then, the proposed algorithm finds the ARW and the GM noise coefficients. ARW and RRW noise parameters are chosen as 0.1 and 0.001 with 10Hz sampling frequency. The Allan variance plots of the generated from the input noise variances and estimated noise parameters are shown in Figure 41. The proposed algorithm finds out the corresponding noise parameters as follows:

Correlation time Tc	= 6397
ARW Noise variance	= 98.7e-003
GM Noise variance	= 1.15e-003

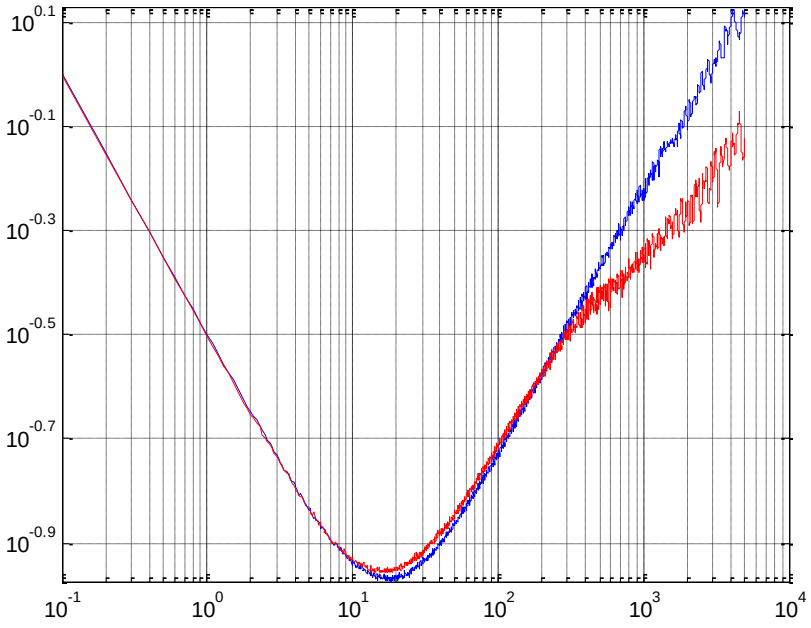

Figure 41: Allan variance of generated (blue) and estimated (red) sensor output

After the performance of the algorithm is shown by the simulated data, a tactical grade inertial measurement unit sensor outputs (i.e. three accelerometers and three gyroscopes), sampled at 10Hz are used to show accuracy of this approach.

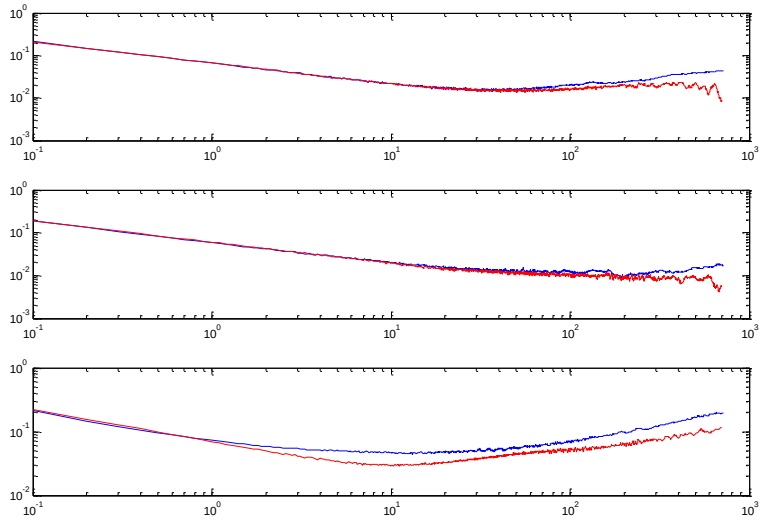

Figure 42: Allan Variance of Inertial Measurement Unit Accelerometer Outputs and the Allan Variance of Estimated Noise at 10 Hz

All of the estimated noise characteristics for the accelerometer outputs are acceptable as shown in Figure 42. On the other hand estimation performances for the first and second accelerometers are better than the third accelerometer. The reason for this is the existence of the bias instability and rate random walk noise sources together at the output of the third accelerometer.

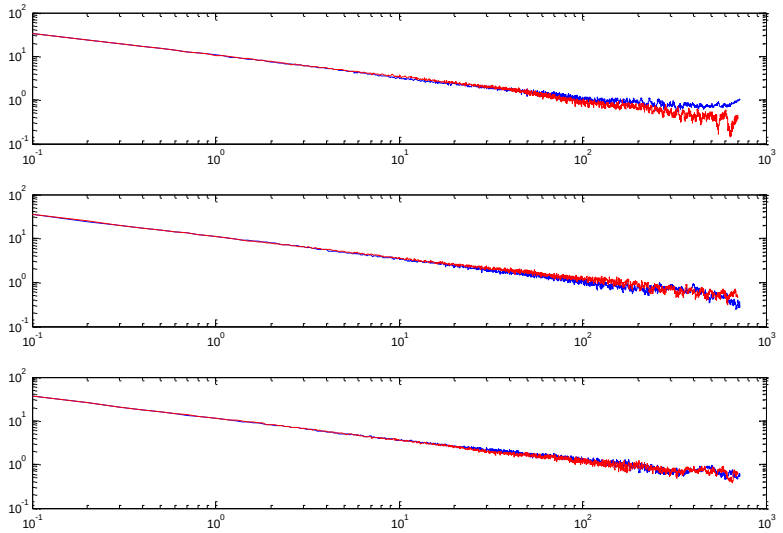

Figure 43:Allan Variance of Inertial Measurement Unit Gyroscope Outputs and the Allan Variance of Estimated Noise at 10 Hz

GM noise does not exist at the gyroscope outputs. All of the estimated gyroscope noise parameters that do not include any GM noise component are shown in Figure 43. As the figures indicate the results are quite satisfactory.

The computations are repeated for IMU2 sensors given in Table XI.

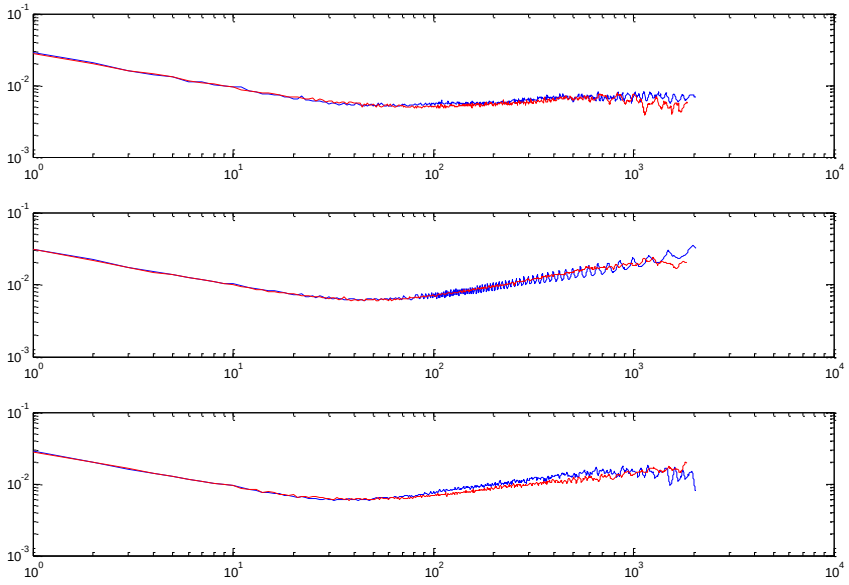

Figure 44: Allan Variance of Inertial Measurement Unit Accelerometer Outputs and the Allan Variance of Estimated Noise at 1 Hz

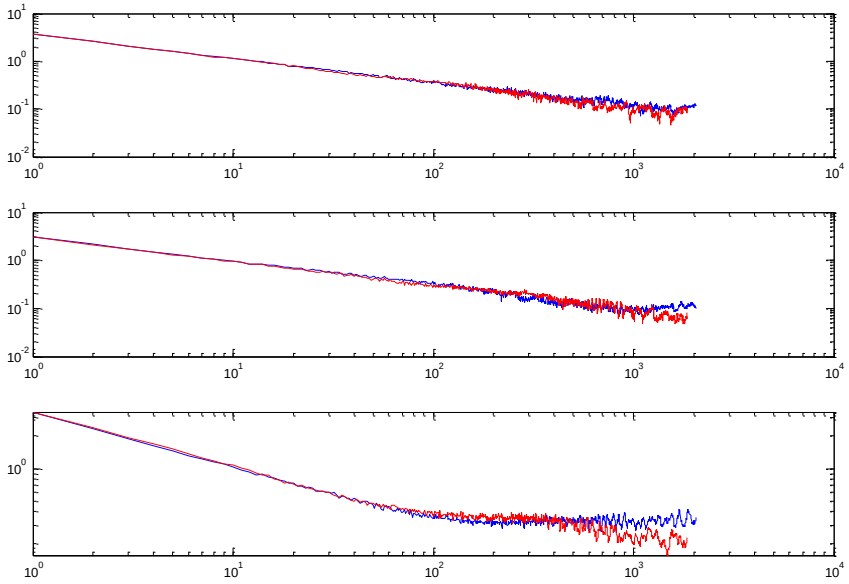

Figure 45: Allan Variance of Inertial Measurement Unit Gyroscope Outputs and the Allan Variance of Estimated Noise at 1 Hz

Estimates of the noise characteristics of both accelerometer and gyroscope outputs of the second inertial measurement unit are even more successful compared to the first one. The comparison of Allan variances of the actual and the simulated data are shown in Figure 44 and Figure 45.

Note that, estimation performance of the proposed algorithm reduces if there exists quantization noise at the sensor output or a low pass filter whose cut off frequency is comparable with the sampling frequency is used at the output stage of the sensor.

8.3 Modeling by Using Two or More GM Noise Sources

The comparison of the Allan variance plots shows some error especially in Figure 42. If the two noise sources, bias instability and rate random walk are approximated with different GM noises this discrepancy may be reduced. Experiments show that the use of more than one GM noise models increases the estimation performance with a slight increase in the computation time. An iterative procedure is applied to compute the two time constants of the two GM noises as well as the other parameters. The procedure keeps the correlation time of one of the GM noises constant and all the other parameters are computed by using the method described previously. The procedure is repeated until convergence by using the optimal correlation time found for the other model. Furthermore the correlation times are constrained in the optimization so that the two correlation time values are considerably different from each other. Golden section selection algorithm is used to determine the time constants.

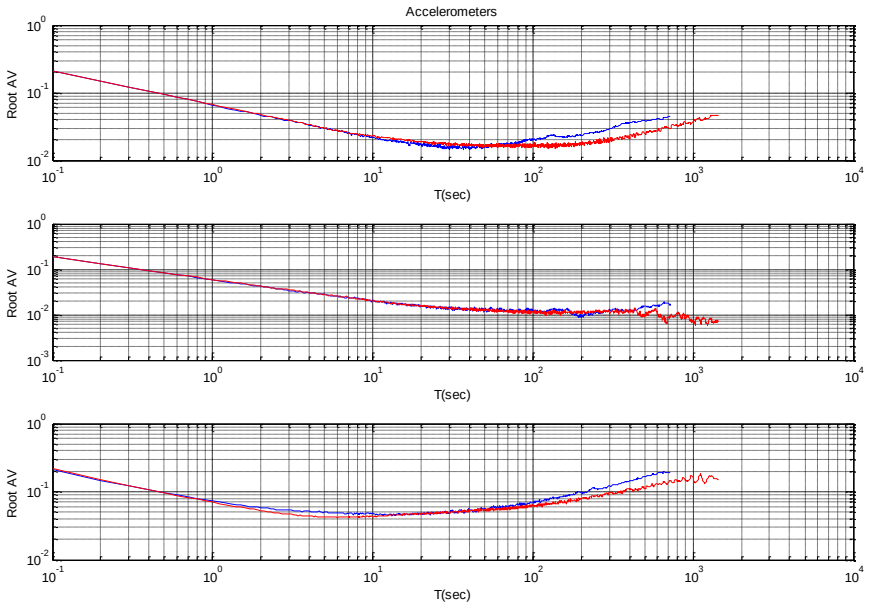

Figure 46: Allan variance of inertial measurement unit accelerometer outputs (blue) and the Allan variance of estimated noises (red) at 10 Hz

Root Allan variance of the original data and deviations from this for the third accelerometer output is given in Figure 42. Figure 46 shows that the use of more than one GM noise in the model improves the performance due to a better characterization of the BI noise source if there are both BI and RRW noises at the sensor output.

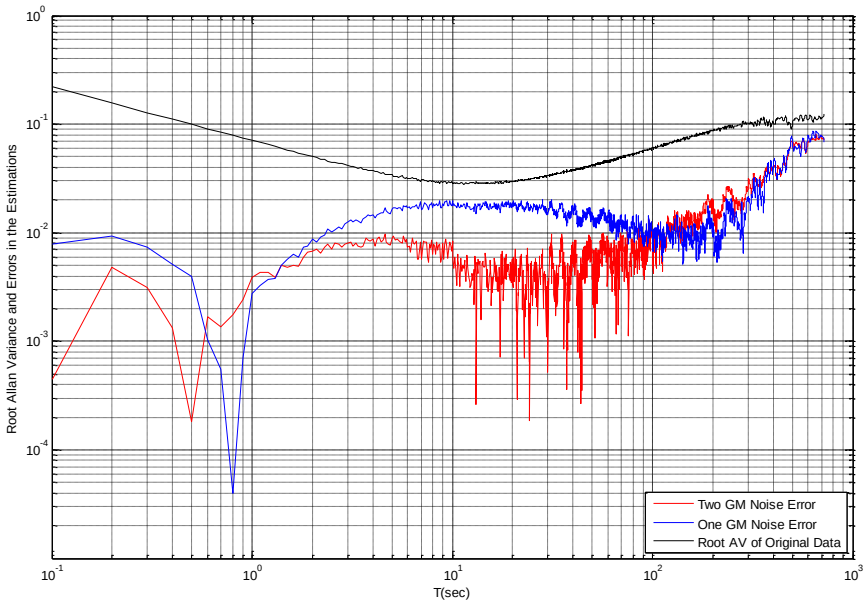

Figure 47: Root Allan variance and Deviations for one and two GM Noise Source in the Model

The same algorithm is applied to the accelerometer output plotted in Figure 32 and explained in Table XI**Hata! Başvuru kaynağı bulunamadı.**. Allan variances of the real data and the estimated noise sources are given in Figure 48. Comparison of the Figures 32 and 48 shows that, the performance of the 3 noise source model is not very different from the full model.

One advantage of the approximation made here is the modeling of a non stationary noise with a stationary one. This approximation is especially useful in the characterization of the BI that is modeled as the output of a filter represented with a non rational transfer function.

In the two noise sources model GM can be used as an approximation of BI or RRW noises. So it gives satisfactory results if the noise consists of only two components: ARW and any of the above mentioned noises. In the three source case ARW and any of the two noises, GM, BI, RRW are modeled satisfactorily. In both of the approaches quantization noise is not included. Existence of quantization may degrade the estimation of the ARW.

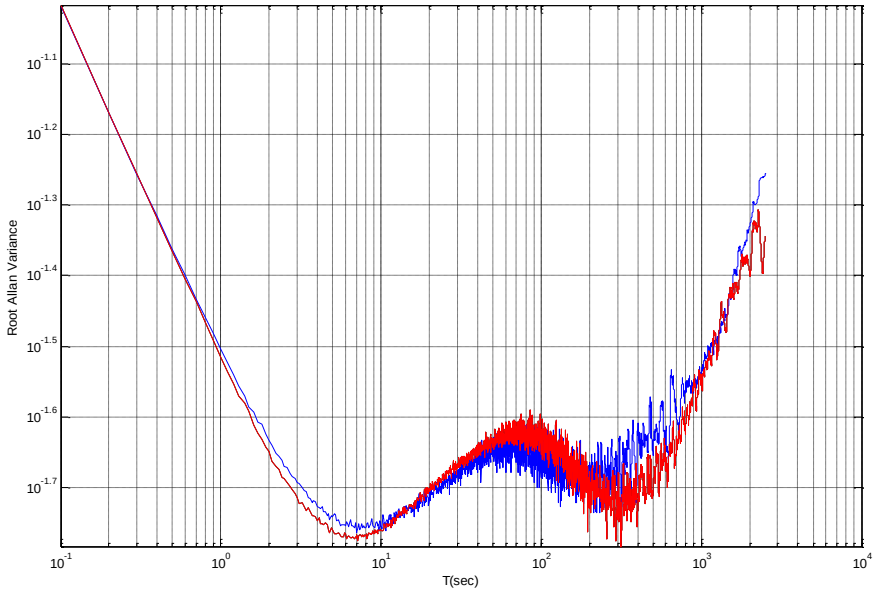

Figure 48: Allan Variance of real sensor output (blue) and estimated sensor output (red)

8.4 Summary

In integrated inertial navigation system design like GPS/INS systems, stochastic errors of the inertial sensors bias term are modeled by using the ARW and GM noise sources, only. The proposed simplified model gives these noise parameters directly and quite accurately. However, in order to obtain good results, there are some limitations related with the sensor output. These limitations are listed below;

- There should not be any quantization noise at the sensor output. This cause the degradation in the estimation of ARW noise covariance.
- The sensor output could not be filtered with a low pass filter whose cut off frequency close to the output frequency of the sensor.

Since the quantization noise of the inertial sensors are almost negligible for modern inertial sensors and low pass filtering at the output stage of the inertial sensors are not common especially for navigation purposes, these limitations are not very important for the proposed algorithm in real life.

CHAPTER 9

CONCLUSIONS

This study aims effective modeling of the stochastic error sources. Our approach is to model different noises as the outputs of different systems driven by white noise. All noise sources are modeled with rational transfer functions except bias instability which requires irrational transfer function representation. Irrational transfer function of BI is approximated by a rational one.

A novel idea of using the difference sequences instead of the original noise sequence is one of the contributions of this study. This approach converts the non-stationary noise to a stationary one. Selection of the lengths of the time intervals for differencing is another important issue in this approach. Long and short time intervals give the parameters of different noise sources. Two different interval length selection procedures, stepwise and quadratic, are applied to the real data. Also Fibonacci numbers are used in a simulation. The results show that stepwise and quadratic are comparable however stepwise is better when the total data length is small. Fibonacci numbers are not as good as in terms of estimation performance.

Using only a few noise source models instead of a full model is another contribution of the paper. In this approach only one or two Gauss Markov noise models are used. The aim is to approximate the low frequency components of the noise by GM. The observations on the real data show the satisfactory performance of this approach. This modeling approach enables the use of the models in the error propagation computations.

When compared with the Allan variance, the advantages of the proposed method are its performance (observed in the simulated data), implementation simplicity and suitability for real time applications. The calculation time is reduced at least 80 times as compared to Allan variance. Furthermore the method is much suitable for an online estimation application.

This method handles most of the stochastic model parameters like Allan Variance, it is much easier to implement and much suitable as an online estimation technique.

This study can be extended to include rate ramp noise source but it requires some modifications in the method so we leave it as a future work. Delay time selection is one of the important parameters of the algorithm that affects both the performance and the calculation time considerably. Selection of the optimum delay times, which is a function of the sensor output and the noise sources, are left as a future work.

Depending on the noise variances optimal interval values that the differences are taken can be determined and used. Initial good estimate of the noise variances results in fixing the interval values that would allow of line computation of the required matrices and this will reduce the real time computation time considerably. Weighting function generally gives good results especially for small data lengths.

Individual noise characterization is one of the applications of this proposed algorithm. If the noise source can be obtained white noise by filtering the transfer function of the form;

$$H(z) = \frac{sr^{\frac{\alpha}{2}}}{\left(1 - z^{-1}\right)^{\frac{\alpha}{2}}}$$

then the proposed algorithm finds both the noise parameters α and the input noise variance, as explained in Chapter 7. Similarly in the same chapter, a method that uses the proposed algorithm to determine the unknown parameters of the GM noise, namely input noise variance and the correlation time, is given. But, noise type, whether GM or not, must be known in order to find out the correct parameters for the noise source.

Online determination of these error source parameters of the inertial sensors using this method will be helpful for both determination of these parameters and usage in integrated inertial navigation system design.

REFERENCES

[1] Elliot R.J., Aggoun L., Moore J.B.; “Hidden Markov Models Estimation and Control” Springer-Verlag, 1995.

[2] Jason J.Ford, Michael E. Evans; “On-line Estimation of Allan Variance Parameters”, Journal of Guidance, Control and Dynamics Vol.23, No.6, Nov-Dec 2000.

[3] IEEE Standard Specification Format Guide and Test Procedure for Single Axis Interferometric Fiber Optic Gyros

[4] Robert J. Elliott, Vikram Krishnamurthy; “Finite Dimensional Filters for ML Estimation of Discrete-time Gauss-Markov Models”, IEEE Proceedings of the 36th Conference on Decision & Control, San Diego, California USA, December 1997.

[5] Quang M. Lam, Nick Stamatakos, Craig Woodruff, and Sandy Ashton; “Gyro Modeling and Estimation of Its Random Noise Sources”, AIAA Guidance, Navigation, and Control Conference and Exhibit 1111- 14 August 2003, Austin, Texas.

[6] N. Jeremy Kasdin; “Discrete Simulation of Colored Noise and Stochastic Processes and $1/f^{\alpha}$ Power Law Noise Generation”, Proceedings of the IEEE, Vol. 83, No. 5, May 1995

[7] R. Narashima, S.B. Rachaiah, R.M. Rao, and P.R. Mukund; “1/f Noise Modeling Using Discrete-Time Self-Similar Systems”, 2003 IEEE

[8] IEEE Standard Specification Format Guide and Test Procedure for Linear, Single-Axis, Non-gyroscopic Accelerometers

[9] Ojeda, L., Chung, H., Borenstein, J.; ”Precision calibration of fiber-optics gyroscopes for mobile robot navigation Robotics and Automation”, 2000. Proceedings. ICRA '00. IEEE International Conference on , Volume: 3 , 24-28 April 2000 Page(s): 2064 -2069 vol.3

[10] Robert J. Elliott, Vikram Krishnamurthy; “New Finite Dimensional Filters for ML Estimation of Discrete-time Gaussian Models”, IEEE Transactions on Automatic Control, Vol, 44, No. 5, May 1999.

[11] Mohammed El-Diasty and Spiros Pagiatakis; “Calibration and Stochastic Modelling of Inertial Navigation Sensor Errors”, Dept. of Earth and Space Science & Engineering, York University, Canada.

[12] Petko Petkov, Tsonyo Slavov; “Stochastic Modeling of MEMS Inertial Sensors”, Bulgarian Academy of Sciences Cybernetics and Information Technologies, Vol. 10, No. 2 Sofia – 2010

[13] Michael S. Bielas; “Stochastic and dynamic modeling of fiber gyros”, SPIE Vol. 2292 Fiber Optic and Laser Sensors XII – 1994

[14] Sameh Nassar, Naser El-Sheimy; “A combined algorithm of improving INS error modeling and sensor measurements for accurate INS/GPS navigation”, GPS Solut (2006) 10: 29–39 DOI 10.1007/s10291-005-0149-3.

[15] M El-Diasty, A El-Rabbany and S Pagiatakis;” Temperature variation effects on stochastic characteristics for low-cost MEMS-based inertial sensor error”, IOP Science Measurement Science and Technology 18 (2007) pg.3321-3328.

[16] Vaibhav Saini, S C Rana, MM Kuber; “Online Estimation of State Space Error Model for MEMS IMU”, Journal of Modelling and Simulation of Systems (Vol.1-2010/Iss.4) pp. 219-225

[17] Ahmed El-Rabbany, Mohammed El-Diasty; “An Efficient Neural Network Model for De-noising of MEMS-Based Inertial Data”, THE JOURNAL OF NAVIGATION (2004), 57, 407–415. f The Royal Institute of Navigation DOI: 10.1017/S0373463304002875

[18] Quang M. Lam, Nick Stamatakos, Craig Woodroff, Sandy Ashton, "Gyro Modeling and Estimation of Its Random Noise Sources", AIAA Guidance, Navigation and Control Conference and Exhibit 1111, 14 August 2003, Austin, Texas.

[19] Yueming Zhao, Milan Horemuz, Lars E. Sjöberg, "Stochastic Modeling and Analysis of IMU Sensor Errors", Archives of Photogrammetry, Cartography and Remote Sensing, Vol.22, 2011, pp. 437-449, ISSN 2083-2214
[20] John H.Wall, David M. Bevly, "Characterization of Inertial Sensor Measurements for Navigation Performance Analysis", Proceedings of the 19th International Technical Meeting of the Satellite Division of The Institute of Navigation (ION GNSS 2006), Fort Worth, TX, September 2006, pp. 2678-2685.
[21] Minha Park, Yang Gao, "Error and Performance Analysis of MEMS Based Inertial Sensors With a Low Cost GPS Receiver", Sensors 2008, 8, 2240-2261